Geophys. J. Int. (2009) **178,** 753–774 doi: 10.1111/j.1365-246X.2009.04164.x

Earthquake cycle in Western Taiwan: Insights from historical seismicity

Sin Mei Ng,[1,2] Jacques Angelier[2] and Chung-Pai Chang[1,3]

[1] *Institute of Geophysics, National Central University, Chungli, Taiwan*
[2] *Observatoire Océanologique de Villefranche-UPMC, Géosciences Azur-OCA, Université de Nice Sophia Antipolis and Institut Universitaire de France, Villefranche/Mer, France. E-mail: jacques.angelier@geoazur.obs-vlfr.fr*
[3] *Centre for Space and Remote Sensing Research, National Central University, Chungli, Taiwan*

Accepted 2009 February 16. Received 2000 January 15; in original form 2008 July 15

SUMMARY

We attempt at providing new insights about the earthquake behaviour in western Taiwan, based on a comparison between historical information and present-day instrumental records. We provide a consistent picture of the earthquake history during the last four centuries and draw some inferences in terms of seismic cycle. Before instrumental seismic observation in Taiwan started at the end of the 19th century, ancient written earthquake records are available from the ancient Chinese governments and the public concerning the 17th, 18th and 19th centuries. Distribution of casualties and property damage, indicating seismic intensity, can be estimated from archives. Using the Central Weather Bureau (CWB) intensity scale we calibrate the intensity–magnitude relationships from the instrumental seismicity recorded from 1995 to 2005, showing that within the range of historical uncertainties and earthquake depths in western Taiwan, 0–40 km, the depth is not critical in these relationships. With estimated intensities, the magnitudes of historical earthquakes can be evaluated based on a single average empirical relationship between M_L, the local magnitude, and I_0, the epicentral intensity: $M_L = 0.08{I_0}^2 - 0.04I_0 + 3.41$. Three types of diagrams are then proposed to describe the historical seismicity. The first type involves simple representation of earthquake events according to time and magnitude. The second type involves cumulative plot of the released elastic energy with time, as calculated from reconstructed magnitudes. The third type of diagram shows the evolution of cumulative seismic strain release with time, based on a Benioff's law indicating that the release of elastic strain related to an earthquake is proportional to the square root of the dissipated energy. These curves highlight inferences of historical seismicity analysis in terms of earthquake frequency and seismic cycle duration in the different segments of the front belt and foreland zones of western Taiwan, with large contrasts suggesting different levels in earthquake hazard.

Key words: Seismic cycle; Palaeoseismology; Earthquake interaction, forecasting, and prediction; Seismicity and tectonics; Asia.

1 INTRODUCTION

Taiwan, located along the western circum-Pacific seismic belt (Fig. 1), is constantly threatened by earthquake hazard. According to the Central Weather Bureau (CWB) 1991–2006 statistics, approximately 18,500 seismic events annually occur, including 1000 felt earthquakes. On average, the whole population experiences 51 events per day; most of them are shallow earthquakes, 0–30 km in depth (Fig. 2a). Earthquakes frequently strike Taiwan because of the geodynamic configuration of the island. East of Taiwan, the Philippine Sea Plate is being subducted beneath the Eurasian Plate along the Ryukyu Trench (Fig. 2b). In the south, the South China Sea of the Eurasian Plate is subducting eastwards beneath the Philippine Sea Plate along the Manila Trench (Fig. 2c). An active collision zone connects these active subduction systems (Fig. 2d). The moving direction of the Luzon arc of the Philippine Sea Plate (Lanhsu GPS station) relative to the Chinese continental margin of the Eurasian Plate (Paisha GPS station) is 306° ± 1° in azimuth, at a rate of 81.5 ± 1.3 mm yr^{-1} (Fig. 1), according to Yu *et al.* (1997, 1999). This complex pattern and fast collision between the Philippine Sea Plate and Eurasian Plate fairly explains the active seismic activity and the orogeny of Taiwan (Suppe 1981, 1984). Hence, the island can be regarded as the product of convergence and subduction-collision processes (Fig. 2d).

Many earthquakes on the island were destructive or devastating: 97 seismic events from 1900 to 2006 were categorized as destructive, many of them having magnitudes greater than, or equal to 5 (Fig. 3). The 1935 Taichung-Hsinchu earthquake (M_L = 7.1,

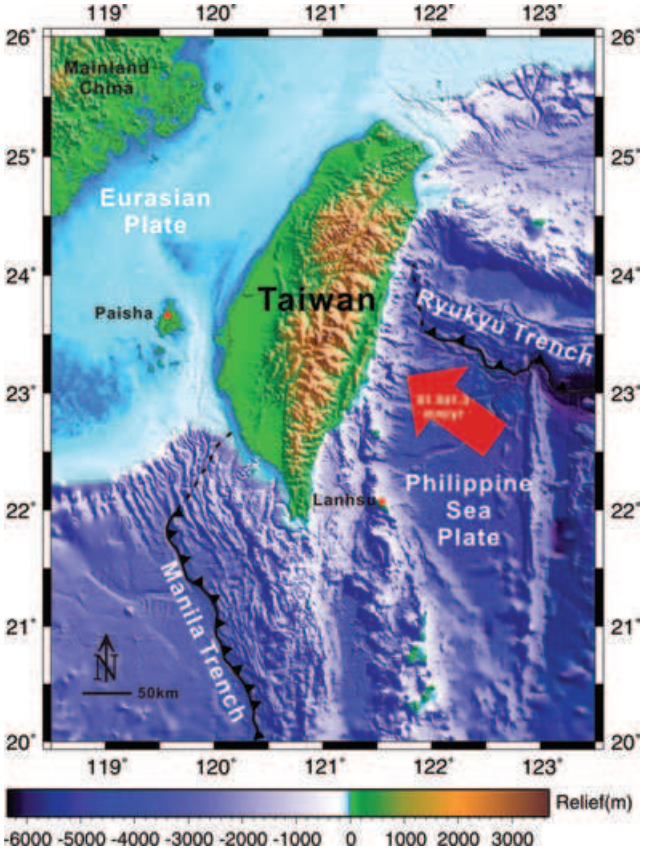

Figure 1. Tectonic framework of Taiwan. Topographic-bathymetric background map made using the GMT software (Wessel & Smith 1995). Thick black lines indicate major subduction boundaries, with triangles on upthrust side (Philippine Sea Plate plunging northward beneath Eurasian Plate along Ryukyu Trench east of Taiwan and Eurasian Plate plunging eastward beneath Philippine Sea Plate along Manila Trench south of Taiwan). Motion of Philippine Sea Plate (e.g. Lanhsu station) with respect to Chinese shelf (Paisha station) indicated by red arrow, with azimuth $306^\circ \pm 1^\circ$ and velocity 81.5 ± 1.3 mmyr^{-1} (Yu *et al.* 1997). Red dots show these two GPS stations.

focal depth 5 km) caused the largest casualties in the 20th century in Taiwan: 3,276 deaths, 12,053 injured, 17,907 houses totally destroyed, 11,405 partially destroyed and 25,376 damaged. Another major destructive earthquake was the 1999 Chi-Chi earthquake ($M_L = 7.3$, focal depth 8 km), which caused 2,456 deaths, 10,718 injured, 53,661 houses totally destroyed and 53,024 damaged.

Two zones are seismically very active, in western and eastern Taiwan (Fig. 2a). Many shallow earthquakes occurred between the Western Foothills and the Coastal Plain (the deformation front). Among these shallow earthquakes, four earthquakes with local magnitudes of 7 or higher occurred in the last century (Fig. 3): 1906 Meishan ($M_L = 7.1$, focal depth 6 km), 1935 Taichung-Hsinchu ($M_L = 7.1$, focal depth 5 km), 1941 Chungpu ($M_L = 7.1$, focal depth 12 km) and 1999 Chi-Chi ($M_L = 7.3$, focal depth 8 km). Such large shallow earthquakes caused large destruction in the highly populated, urbanized areas of western Taiwan.

In this study, we consequently focus on western Taiwan, where the largest cities are located. Approximately 95.6 per cent of the Taiwan population live in our investigated regions, with more than one third in six major cities (Taipei, Hsinchu, Taichung, Chiayi, Tainan and Kaohsiung, from North to South), according to statistics from the Population and Density of Urban Planning 2007, Construction and Planning Agency, Ministry of the Interior (MOI).

The aim of this paper is to evaluate the seismic cycle, that is, the recurrence time interval of major earthquake events in western Taiwan, based on the analysis of the available information issued from historical record since nearly four centuries. No valuable information about earthquakes exists in Taiwan for the historical period prior to Chinese settlement during the Ming Dynasty. As a major difficulty in the study, we need to reconcile the historical information of the 17th, 18th and 19th centuries, which is essentially qualitative, with the abundant and accurate information of the more recent instrumental period. On one hand, it is appropriate for comparison purposes to consider this accurate information in terms of locations, magnitudes and intensities. On the other hand, obtaining a homogeneous database over four centuries precludes direct integration of accurate seismological information. For this reason, we address the problem of intensity–magnitude relationships, to evaluate the relative importance of old and recent earthquakes and give them appropriate weight in the total record.

For many historical earthquakes, especially before the 20th century, the information about intensity is scarce and imprecise and the location of epicentre is unknown. Thus in most cases we could not reliably determine the distribution of intensities and rigorously evaluate the epicentral intensity for these ancient earthquakes according to the Bakun and Wentworth's method (Bakun & Wentworth 1997; Bakun 2005). To process in an homogeneous manner all the data, we addressed the problem of intensity–magnitude relationships using a simpler approach, as explained in Section 3.

2 SEISMIC RECORDS IN TAIWAN

Two types of seismic records, historical and instrumental in nature, co-exist in Taiwan. Over 100 yr had elapsed since instrumental seismic observation started at the end of the 19th century. A large quantity of ancient written earthquake records predating the appearance of instrumental records is available, from both the ancient Chinese governments and the public. Written reports can be found starting from the beginning of the 17th century and lasted for nearly 300 yr (Hsu 1983a; Cheng & Yeh 1989). They include official reports from local governments to imperial Chinese governments, local government reports, descriptions in Dutch travel books, etc. To no amazement, most of these historical documents record only destructive earthquakes. After the installation of seismographs, a large quantity of large and small seismic events was recorded. In any study of the earthquake activity, it is thus indispensable to separately consider different historical periods as a function of the sensitivity of available instruments. From the analysis of instrumental records, four stages of instrumental seismic observation can be identified: early (1900–1935), intermediate (1936–1972), Taiwan Telemetered Seismographic Network (TTSN) (1973–1991) and CWBSN (1992–present) stages of instrumental seismic observation (Shin & Chang 2005 and Fig. 4).

2.1 Early stage (1900–1935)

The installation of the first Gray-Milne seismometer in December, 1897 in Taipei marked the official beginning of instrumental seismic observation in Taiwan. This type of seismometer was later installed in Tainan, Penghu, Keelung, Taichung, Taitung and Hengchun. Omori type of seismometers was later added. Before 1907, only first arrival time and intensity could be recorded; after 1908, the epicentral location was also calculated. In 1928, seismometers of Wiechert type, with Omori and strong motion seismometers, were installed

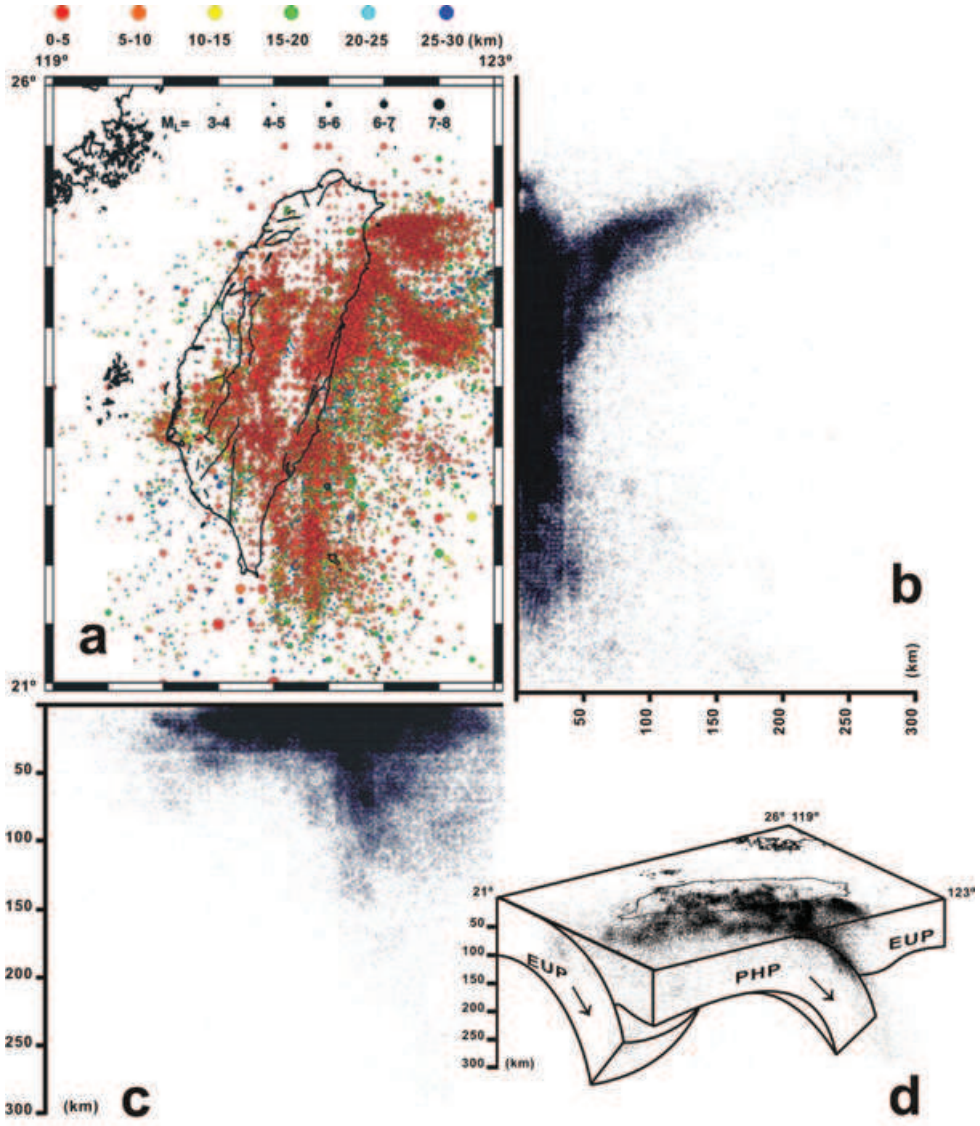

Figure 2. Distribution of earthquakes, 1900–2006, in and around Taiwan. Seismic data from the CWB, Taiwan (http://www.cwb.gov.tw/). (a) Map of epicentres. Colour codes refer to earthquake depths, as indicated above the map. Only shallow earthquakes, 0–30 km deep with magnitudes $M_L \geq 3$, are plotted. Dot size increases with magnitude (with scale indicated inside the map). Black solid lines on the island are major active faults. (b and c) Cross-sectional views of earthquakes with magnitudes $M_L \geq 3$ at all depths (0–300 km), as seen from East (b) and South (c), with same scale as in the map. (d) Perspective view of Taiwan, with the same earthquakes as in cross-sections. Trend and elevation of line of sight are, respectively, 306° (same as plate convergence direction) and 20°. EUP and PHP, Eurasian Plate and Philippine Sea Plate, respectively.

in Taipei, Tainan, Penghu, Hualien, Alishan, Taitung, Hengchun, Kaohsiung and Taichung. The earliest available seismic data started from May 15, 1900 and no magnitude smaller than or equal to 4 could be recorded during 1900–1935 (Fig. 4, I). The focal depth determination was bad, with few 10 or 20 km depths and a 0 km depth being assigned to most events.

2.2 Intermediate stage (1936–1972)

The occurrence of the Taichung-Hsinchu destructive earthquake in 1935 (Fig. 3) marked the transition between the early and intermediate stages of seismic observation. This disastrous, $M_L = 7.1$ earthquake caused the largest casualties in the 20th century in Taiwan. As a major seismological improvement after the earthquake (Fig. 4, I), the number of stations increased with the addition of Hsinchu, Ilan, Dawu and Chengkung stations. Significant amounts of magnitude 4 earthquakes could then be recorded and focal depth could be calculated in more detail. Before the end of the Japanese occupation in 1945, there were totally 16 seismic stations on the island. At the end of the Second World War, the seismic observation nearly ceased from March 1945 to January 1946. This period is regarded as the dark years of seismic observation in Taiwan, because the seismometers were getting obsolete or damaged. New strong motion seismometers and accelerometers were added after the occurrence of large earthquakes in 1951 in eastern Taiwan. In 1963, with the help of the United States Coast and Geodetic Survey, the CWB chose Anpu, Taipei to install a World-Wide Standardized Seismograph Network (WWSSN) station. Until 1968, the seismic network of CWB totally included 16 stations throughout the

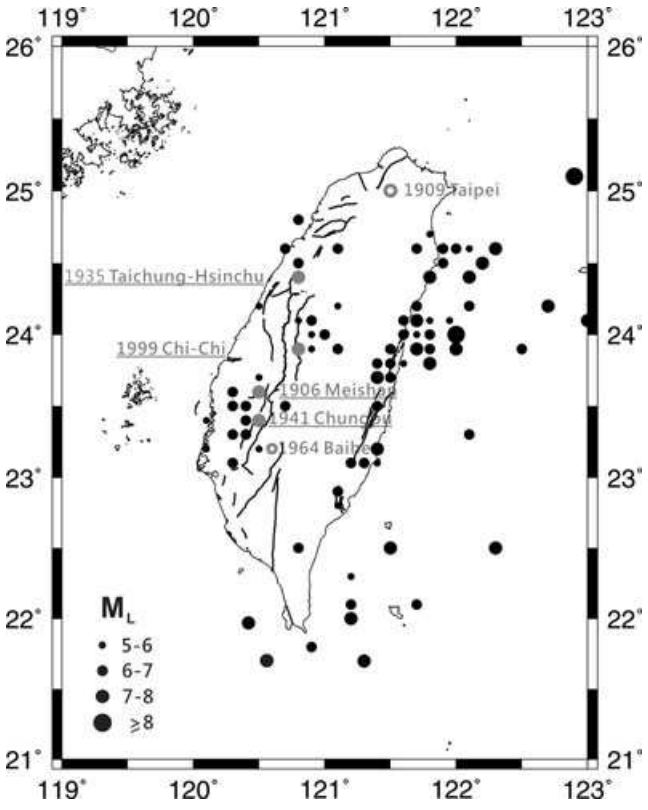

Figure 3. Map of epicentres of destructive earthquakes, $M_L \geq 5$, in Taiwan from 1900 to 2006. The four solid grey dots indicate examples of the largest instrumentally recorded onland destructive earthquakes: 1906 Meishan ($M_L = 7.1$, depth 6 km), 1935 Taichung-Hsinchu ($M_L = 7.1$, depth 5 km), 1941 Chungpu ($M_L = 7.1$, depth 12 km) and 1999 Chi-Chi ($M_L = 7.3$, depth 8 km). Two open grey circles refer to large earthquakes mentioned in text: 1909 Taipei ($M_L = 7.3$, depth 80 km) and 1964 Baihe ($M_L = 6.3$, depth 18 km). Black solid lines on the island are major active faults. Data extracted from CWB website (http://www.cwb.gov.tw/).

island (Anpu, Taipei, Hsinchu, Taichung, Chiayi, Alishan, Penghu, Yushan, Tainan, Kaohsiung, Hengchun, Ilan, Hualien, Chengkung, Taitung, Dawu) and one station in the neighbouring Lanhsu Island to the Southeast.

Although following Yeh *et al.* (1994) we consider herein two stages of seismic observation, early and intermediate, the Weather Central Bureau regarded these two stages as the first stage ('mechanical observation' stage), because the whole seismic network was mainly based on mechanical seismographs with few magnetic types at later time. No matter how the earliest instrumental seismic observation was categorized, it definitely came to the end when the Taiwan Telemetered Seismographic Network (TTSN), started operating in 1973.

2.3 TTSN stage (1973–1991)

The occurrence of the Baihe earthquake ($M_L = 6.3$) in 1964 (Fig. 3), which killed 106 people and 10,924 houses totally destroyed, accelerated the modernization of seismic observation because both the government and the public were threatened by earthquake hazard. Since 1971, the preparatory work for the establishment of the Taiwan Telemetered Seismographic Network, TTSN, started. Between 1972 and 1973, the Institute of Earth Sciences, Academia Sinica—albeit not yet formally established at that time—completed the establishment of TTSN and the Strong Motion Accelegraphic Network, SMA (Fig. 4, II). Since then, TTSN and SMA have started a new milestone in seismic observation since the systems involved automatic, all-weather, real-time seismic observation. The TTSN had 25 stations and sensors used were L4C by Mark or SS-1 by Kinematric. The coverage area was 21°–26°N and 119°–123°E. Seismic data from all stations were simultaneously received by telephone or wireless through a centralized receiving system in Taipei. Hence, this network significantly enhanced the accuracy of earthquake location. Moreover, the location of the TTSN stations was strictly chosen on the bed-rock sites and the number of the stations increased with highly sensitive sensors. As a consequence of better detecting ability, the number of recorded seismic events increased by more than ten times (Fig. 4). Magnitudes smaller than 1 could be recorded, albeit in very small numbers. The determination of focal depths was significantly improved and the process of earthquake location was computerized or digitized since June 12, 1987.

2.4 CWBSN stage (1992–present)

The Seismological Centre, CWB was established in 1989 and one of its major aims was to form a complete seismic observation network in Taiwan. The Central Weather Bureau Seismic Network (CWBSN), gradually developed under this vision. Besides 25 TTSN and 19 original stations, 31 more stations were added to form a 75-station network. In each station, S-13 and strong motion seismographs were installed. The earthquake location time was shortened from more than 10 min to 3–5 min. According to the statistics, over a thousand or several thousands events per month could be monitored, as compared to 300–400 events before the upgrade of the network. In recent years (after 2000), the total number of magnitude 1–2 earthquakes was getting higher than the number of magnitude 2–3 earthquakes (Fig. 4), as a consequence of the increasing detecting capacity of the network.

In mid-1992, the Institute of Earth Sciences, Academia Sinica started preparing the establishment of the Broadband Array in Taiwan for Seismology, BATS (Kao *et al.* 2001; Kao & Jian 2001). Broadband seismographs (Streckeisen STS-1 or STS-2 in type) could record lower frequency of seismic waves, as a major contribution to seismotectonic research in Taiwan. The BATS network was designed with 15 permanent stations and 15 portable units, covering an area of about 350 × 400 km. The earthquake parameters in the Taiwan region were routinely estimated, including the eastern offshore area. Thus, the installation of the BATS and CWBSN networks, together with the Taiwan Strong Motion Instrumentation Program (TSMIP) and the Earthquake Rapid Reporting System (ERRS) marked the onset of the present-day period of seismic observation in Taiwan (Fig. 4).

3 MAGNITUDE ESTIMATES

Magnitude determination is a common problem while establishing seismic catalogues. In previous studies of historical earthquakes, several authors aimed at determining magnitudes from the only information available for ancient earthquakes, which is mainly related to the damage produced by ground acceleration: that is, seismic intensity.

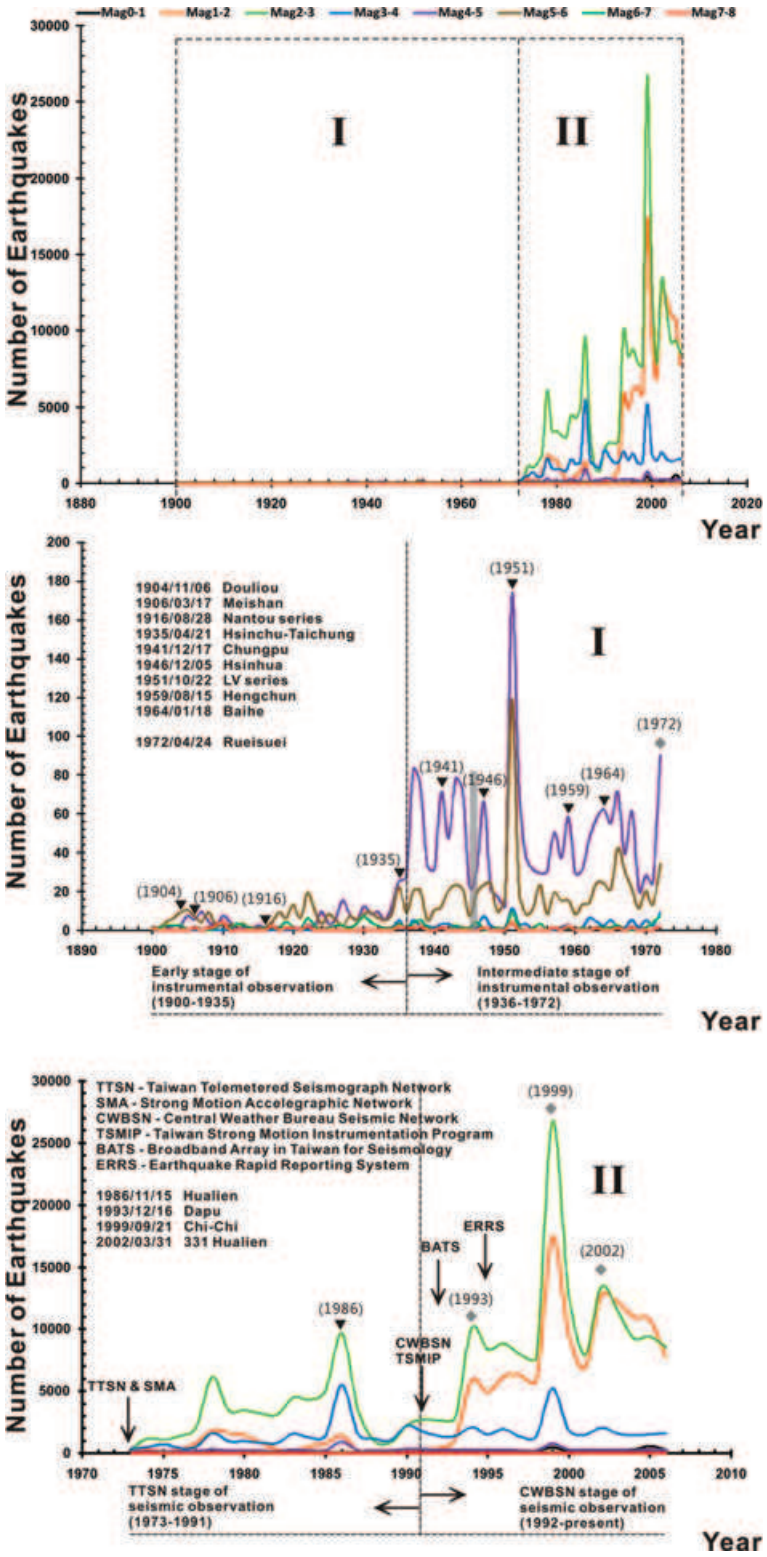

Figure 4. Temporal evolution of seismic records in Taiwan, 1900–2006. Eight coloured lines indicating various magnitudes (0–1, 1–2, 2–3, 3–4, 4–5, 5–6, 6–7, 7–8, with colour code in top diagram) show changes in the number of recorded earthquakes as a function of time. (I) From 1900 to 1972. The earliest available seismic data started from 1900 May 15. The Taichung-Hsinchu earthquake (1935) separated the early (1900–1935) and intermediate (1936–1972) stages of instrumental seismic observation. A gap in earthquake observation between March, 1945 and January 1946, as a consequence of the Second World War, is indicated by grey stripe. (II) From 1973 to present. The installation of the Taiwan Telemetered Seismograph Network (TTSN) in 1973 by Academia Sinica was a milestone in seismic observation through time (the TTSN stage, 1973–1991). The development of the Central Weather Bureau Seismic Network (CWBSN) marked the modern CWBSN stage (1992–present).

3.1 Magnitudes and intensity scales

In 1935, C.F. Richter introduced the concept of earthquake magnitude (Richter 1935). The magnitude of an earthquake was originally determined from the logarithm of the amplitude of waves recorded by Wood-Anderson seismograph. A number of other logarithmic magnitude scales for earthquakes appeared later. All magnitude scales are of the following form:

$$M = \log_{10}\left(\frac{\mathrm{A}}{T}\right) + q(\Delta,h) + a \quad (1)$$

where M is the magnitude, A the maximum amplitude of the wave (in 10^{-6} m), T the period of the wave (in seconds), q is a function correcting for the decrease of amplitude of the wave with distance from the epicentre and focal depth (Gutenberg & Richter 1956a), Δ the angular distance from seismometer to epicentre (in degrees), h the focal depth of the earthquake (in kilometers), and a an empirical constant. New magnitude scales (Table 1, including eqs 2–6) have been introduced since the concept of earthquake magnitude first appeared.

To a certain extent, multiple scales reflect the difficulty of magnitude determinations and the need for accurately expressing the size or strength of an earthquake. The problem is still more difficult for ancient earthquakes, because of very large uncertainties. The only available information consists of intensity estimates obtained based on records of damage that are often inaccurate or incomplete. Evaluating the earthquake intensity provides a simple, empirical way of measuring or rating the effects of an earthquake at different sites. In the absence of instrumental information, only intensity evaluation could be applied to ancient earthquakes, as shown by Tsai (1985). The technique for evaluating the intensity of an historical earthquake includes the following steps (Figs 5b and d).

(1) At each location where the earthquake has been felt, a numeral is assigned to describe the earthquake effect (0–7 according to the latest CWB intensity scale, I-XII according to the Mercalli intensity scale).

(2) A contour map is drawn, to locate the zones with similar effect.

(3) The earthquake epicentre is assumed to be in the region of maximum intensity.

(4) This earthquake is characterized by the maximum intensity, I_0, as the largest Roman numeral assigned (VI for the examples shown in Fig. 5).

Following Tsai (1985), we adopted the CWB intensity scale rather than the Mercalli intensity scale. The main reason was that this CWB scale, which is simpler, better fits the lack of accurate information about intensities for ancient earthquakes in Taiwan. The hand-depicted isoseismal maps (as in Fig. 5) are no longer in use. From accurate measurements of the peak ground acceleration (PGA) with modern seismographs, isoseismal maps (Fig. 6) are systematically produced (Hsiao 2007). According to this author, the maximum PGA recorded by the real-time strong-motion stations can be used as follows to obtain the intensity in Taiwan, I_T.

$$I_T = 2.00\log_{10}(\mathrm{PGA}) + 0.70. \quad (7)$$

3.2 Local intensities and intensity at epicentre

Four examples of Taiwan earthquakes in 1999 and 2000, with local magnitudes decreasing from 7.3 to 5.0, are shown in Fig. 7 to illustrate the relation between intensity and epicentral distance. According to a method described by Bakun and Wentworth (1997) and Bakun (2005), such an analysis allows determination of the intensity at epicentre. We found that a decreasing exponential law well accounts for the distribution of intensities as a function of distance to epicentre. The interest of this method clearly appears in Fig. 7b: whereas the largest recorded intensity was 6, the data distribution suggests that intensity 7 was reached at the epicentre. This method will be applied to the recorded intensities of the instrumental period in a future paper, starting from the CWB records available since 1995. However, we did not use it in a systematic way in the present paper because we intended to analyse all known historical earthquakes, including those for which the appropriate information was not available.

3.3 Application to Taiwan earthquakes

The epicentral locations and magnitudes of most historical earthquakes are poorly known. However, some locations and magnitudes have already been estimated by Lee *et al.* (1976), Hsu (1983b) and Tsai (1985). The methods for magnitude evaluation adopted by these three authors can be summarized as follows.

Initially, Lee *et al.* (1976) did not estimate the magnitude of historical earthquakes but codified the data previously published in the 'Catalog of Chinese earthquakes' (Academia Sinica 1970a). They produced a summary in a form suitable for computer input and they brought attention to the western scientific world concerning the existence of ancient Chinese earthquake data, following the effort made by Academia Sinica (AS) in Peking (Beijing) in the 1950s, 1960s and 1970s. Because of the absence of detailed explanation, there is however no simple way to evaluate the methods that were used. In the paper by Lee *et al.* (1976), the magnitude, M (without

Table 1. A number of logarithmic magnitude scales (Eqs 2–6) for earthquakes: surface-wave magnitude, M_s, body-wave magnitude, M_b, and moment magnitude, M_w.

Surface-wave magnitude, M_s (eq. 2)	$M_s = \log_{10}(A/T)_{max} + 1.66\log_{10}\Delta + 3.3$ where $(A/T)_{max}$ refers to the horizontal component of Rayleigh waves, $T = 20 \pm 3$ sec (Båth 1981)	For shallow focus (<50 km) teleseismic earthquake ($20^\circ < \Delta < 160^\circ$) Δ, angular distance from seismometer to epicentre (in degrees)
Body-wave magnitude, M_b (eq. 3)	$M_b = \log_{10}(A/12) + 0.01\Delta + 5.9$ (Gutenberg 1945)	shallow-focus earthquakes for P, PP, and S waves of 12-second period
Body-wave magnitude, M_b (eq. 4)	$M_b = \log_{10}(A/T)_{max} + q(\Delta,h)$ Gutenberg and Richter (1956a) (more generally used today than eq. 3) $q(\Delta,h)$ is defined in text	$(A/T)_{max}$ is determined for all waves for which calibrating functions are available (PZ, PH, PPZ, PPH, SH)
Moment magnitude, M_w (eq. 5)	$M_w = (2/3)\log_{10}M_o - 10.7$, where M_o, the seismic moment, is defined by $M_o = \mu DS$ (Eq. 6) (Kanamori 1977, 1978; Båth 1981)	In Eq. 6, μ is the shear modulus or rigidity, S the surface area of the fault and D the average displacement on the fault.

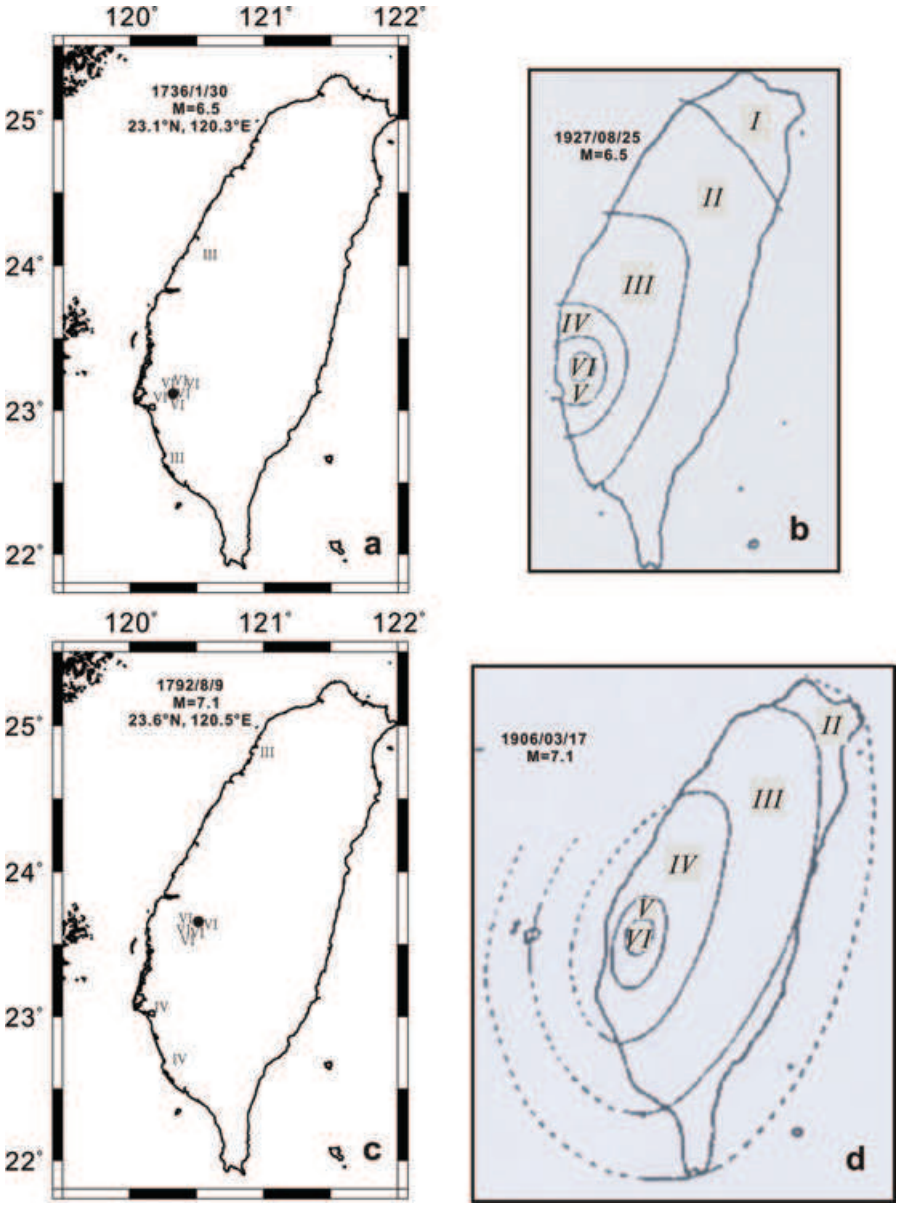

Figure 5. Two examples of determinations of epicentres and magnitudes of historical earthquakes (adapted from Tsai 1985). Epicentres and magnitudes of the 1736 January 30 and 1792 August 9 earthquakes (a and c, on left) were determined by comparing their intensity distribution with the isoseismal maps of similar, instrumentally recorded earthquakes (b and d, on right): the 1927 August 25 ($M = 6.5$) and 1906 March 17 ($M = 7.1$) earthquakes.

specified type), was determined by using the following formula:

$$M = 0.58I_0 + 1.5, \tag{8}$$

where I_0 is the epicentral intensity. The magnitude of a vast quantity of historical Chinese earthquakes from 1177 B.C. to 1899 A.D. cannot simply be determined using a single law that does not take major parameters such a focal depth into account, so that Eq. (8) is regarded as a first approximation. Even the intensity scale adopted for ancient earthquakes was somewhat uncertain, although Lee *et al.* (1976) suspected that it was that from Hsieh (1957), similar to the modified Mercalli scale. Moreover, the adjustment method is unknown in source materials (Academia Sinica 1970a,b, 1974) and Lee *et al.* (1976) did not discriminate between the different types of magnitudes.

Later, depending on the available historical information, Hsu (1983b) used one of the following four methods to estimate the magnitude of twenty-seven earthquakes in Taiwan, known from the Ming and Ching Dynasties earthquake study of Hsu (1983a). First, according to the maximum epicentral intensity method, the magnitude could be determined from the relation between earthquake magnitude, M, and maximum epicentral intensity of Richter (1958), I:

$$M = \frac{2I}{3} + 1. \tag{9}$$

Second, using the radius of the felt distance γ, the following formulae of Gutenberg and Richter (1942,1956b) were adopted by Hsu (1983b):

$$\gamma = 2.3(M - 1.3)^3 - 1.7; \quad M = -3.0 + 3.8 \ \log r;$$
$$r = 1.4(M - 0.614)^3 \tag{10}$$

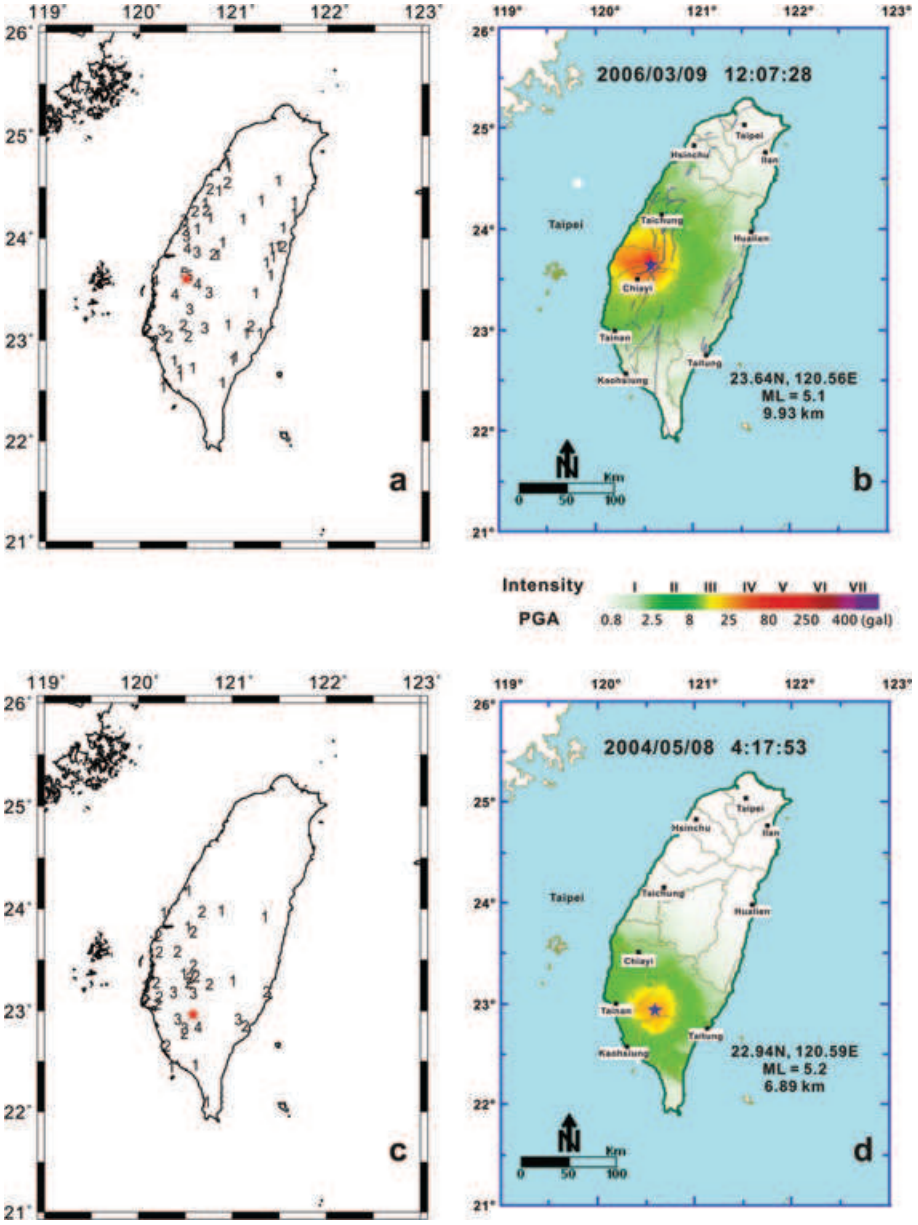

Figure 6. Relationship between intensity and peak ground acceleration (PGA) in Taiwan. Example of two earthquakes, 2004 May 8 and 2006 March 9, with local magnitudes 5.2 and 5.1, respectively, (modified after CWB, http://www.cwb.gov.tw/). (a and c) intensity maps. Red stars indicate epicentres of the earthquakes and numbers indicate intensities recorded at stations (PGA values recorded in stations were used to determine intensities). (b and d) corresponding 'shake maps' provided by the CWB. For the processing method the reader is referred to Hsiao (2007).

where M is the magnitude and r is the radius (in kilometres). Third, the same author also used a formula giving the magnitude as a function of the Kawasumi's Intensity Magnitude, M_k, a value based on evaluation of the intensity 100 km away from the epicentre (Kawasumi 1943; see also Wang 1992):

$$M = 4.85 + 0.5M_k. \quad (11)$$

Fourth, the extent and area of damage, the number and duration of aftershocks, the characteristics of crustal deformation or tsunami, and the magnitude of instrumental earthquakes when available, were considered. Hsu (1983b) estimated the location of the epicentre as the area where the maximum damage occurred and the intensity scale used was the CWB intensity scale, with the Modified Mercalli Seismic Intensity Scale as a reference. The above examples, from Hsu (1983b), illustrate the complexity of the available magnitude evaluations concerning historical earthquakes, without any unique or standard method.

Finally, Tsai (1985) estimated the intensity at each damaged area using the CWB intensity scale and the source materials from Fang (1969) and Hsu (1983a). Then the geographical distribution of intensity of each major historical earthquake could be drawn (Fig. 5a). The isoseismal map of a more recent, instrumentally recorded earthquake was used as a reference for comparison with each historical intensity map; for instance, Tsai determined magnitudes 6.5 and 7.1 for two major earthquakes in 1736 and 1792, based on comparisons with earthquakes in 1927 and 1906, respectively (Figs 5b and 5d). The magnitude of 11 major historical earthquakes from 1736 to 1882 could thus be determined (Tsai 1985).

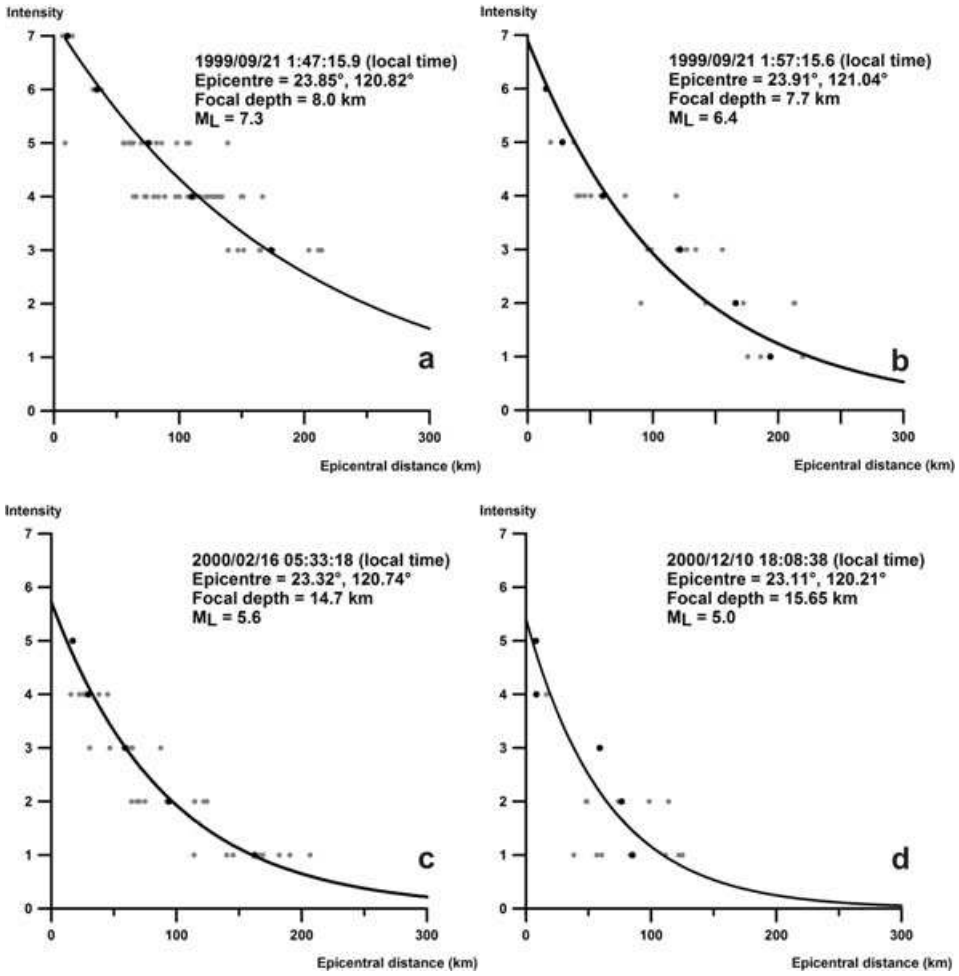

Figure 7. Relationships between intensity and epicentral distance. Four examples of Taiwan earthquakes in 1999 and 2000 (including the main shock of Chi-Chi earthquake, $M_L = 7.3$), with magnitudes decreasing from 7.3 to 5. The grey dots refer to individual measurements. The black dots indicate the average epicentral distance for each intensity. The black solid line is the best-fitting curve obtained with the five (a, c and d) or six (b) average values. Note that the expected intensity at epicentre may be significantly larger than the closest recorded intensity (b and c).

It is worth noting that the accuracy of an isoseismal map of an instrumental earthquake might be poor and the number of intensities actually estimated for each historical earthquake was generally too small to determine a well-defined distribution throughout the island. Thus, using a small area of estimated intensity for comparison with an isoseimal map of the island did not provide a good evaluation of its accuracy. The variety of methods that were employed by authors to evaluate the magnitude of historical earthquakes in Taiwan also precluded consistent syntheses. One cannot conclude that Lee *et al.* (1976) have completed the task of estimating intensity or magnitude of historical earthquakes. Too many critical parameters, such as the focal depth, remain unconstrained by the data and could not be documented. Even the accuracy and reliability of each method is difficult to evaluate. However, because the historical data mentioned above provide a unique source of information about the ancient earthquakes of the last three centuries in Taiwan, despite ambiguities it is necessary to use this information to reconstruct the earthquake evolution.

3.4 Insights from present-day seismicity

The magnitude is important in that it reflects the dissipated energy of earthquakes, a critical property in the earthquake cycle. Because the intensity provides the only access to magnitude evaluation for ancient earthquakes, we undertook a systematic analysis of the relationships between the intensity and magnitude, as documented by modern instrumental records. We considered the maximum intensity, I_0, and the local magnitude, M_L, indicated by the records of the CWB for the earthquakes of the period from 1995 to 2005 in western Taiwan. Note first that the magnitudes displayed by the CWB are local magnitudes (M_L), so that the relationship between M_L and M_W, the moment magnitude, must be taken into account. This problem of relationships between different magnitudes has been discussed, for the Taiwan earthquakes, by Wang (1992) and Chang (2002). Wang (1992) concluded that a good approximation is represented by the following formula:

$$\log_{10} M_o = (14.571 \pm 1.683) + (1.598 \pm 0.236) M_L, \qquad (12)$$

where the seismic moment, M_o, allows determination of the moment magnitude as mentioned earlier (eqs 5 and 6 in Table 1).

The results of our analysis are summarized in Table 2. We considered the usual earthquake depth range for most earthquakes in western Taiwan, that is, from the surface to 40 km depth. Then we examined the CWB data and we determined through linear regression analysis, for each depth class of 10 km, the relationship between the recorded maximum intensities and the calculated

Table 2. Summary of empirical relationships between magnitude and intensity, as determined at different depth ranges from the CWB earthquake records from 1995 to 2005 in western Taiwan. *D*, depth range. N, number of earthquakes considered. The parameters *a* and *b* of the relationship $M_L = aI_0 + b$ obtained by linear regression are shown, as well as the linear regression coefficient R_L. The last column, with regression coefficient R_p, refers to degree 2 polynomial adjustment of Fig. 8.

D (km)	*N*	*a*	*b*	R_L	R_p
0–10	354	0.43	2.87	0.68	0.69
10–20	351	0.45	2.54	0.67	0.71
20–30	107	0.44	2.86	0.68	0.69
30–40	14	0.52	2.79	0.75	0.76

magnitudes, resulting in the four graphs of Fig. 8. From 1995, the CWB has built a seismic catalogue using the short-period and PGA data, and we used the data collected from 1995 to 2005. As similar curves are obtained for the four depth classes, it appears that for the crustal earthquakes of western Taiwan the focal depth is not a key factor affecting the result of the linear regression. Note however that large magnitudes are poorly represented, with few intensities reaching 6 above 20 km depth, and no intensity larger than 5 below. The linear regression is thus only valid for relatively low intensities and magnitudes. Note also that the relationship (8) from Lee *et al.* (1976) provides too low magnitude values as a function of intensity (Fig. 8).

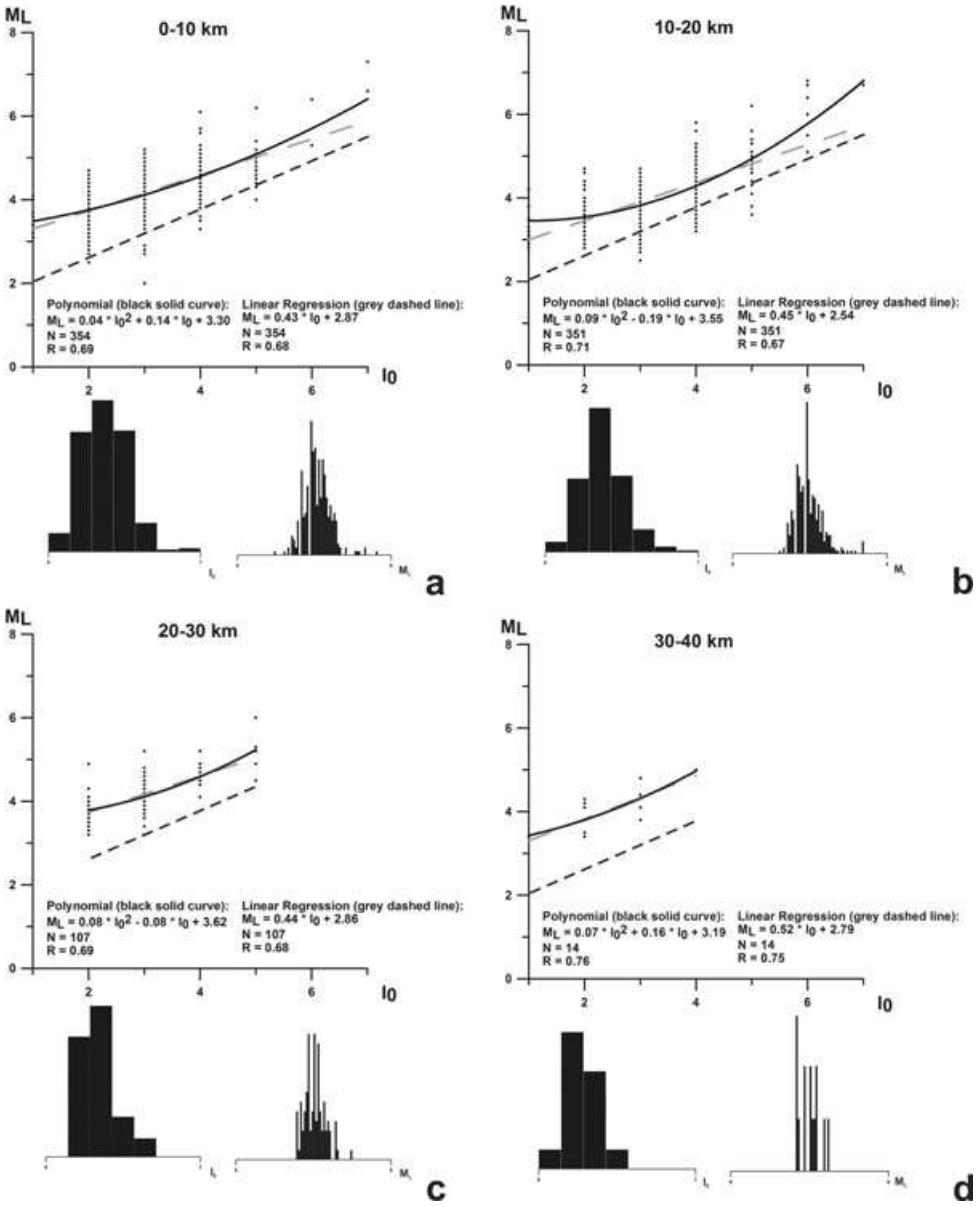

Figure 8. Relationships between local magnitude, M_L, and maximum intensity, I_0, within four depth ranges from 0 to 10, 10 to 20, 20 to 30 and 30 to 40 km depth in western Taiwan. Data from the CWB, recording period from 1995 to 2005. Black dashed lines (with short dashes) refer to the linear relationship between intensity and magnitude, $M = 0.58I_0 + 1.5$, previously provided by Lee *et al.* (1976) for Chinese earthquakes. Two adjustments were performed this paper, using all data (shown as points) and equal weighting for each intensity class. Grey dashed lines (with long dashes) result from linear regression. Black, parabolic solid curves refer to adjustment of a polynomial function of degree 2. See also Table 2. The two histograms below each diagram show the corresponding distributions of maximum intensities (on left, from 1 to 7) and local magnitudes (on right, from 0 to 8).

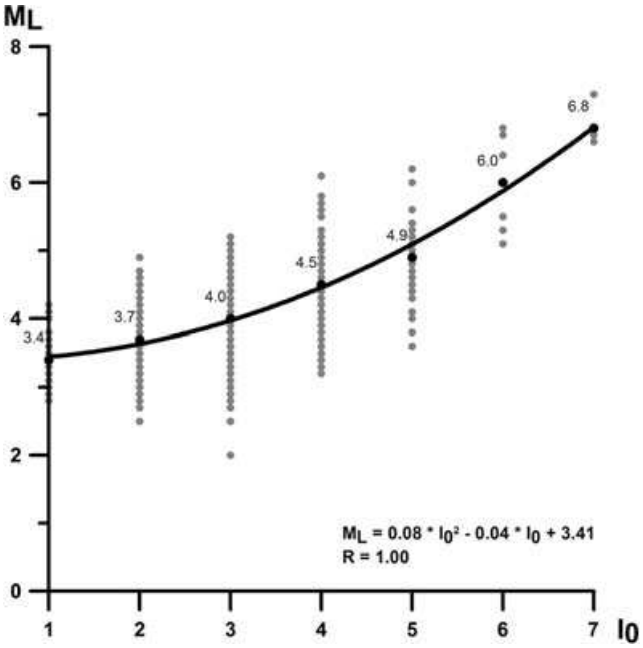

Figure 9. Relationship between local magnitude, M_L, and maximum intensity, I_0. Adjustment using a polynomial function of degree 2, based on the data recorded by the CWB for the period 1995–2005. Grey dots indicate individual couples of measured values M_L and I_0 while black dots correspond to average magnitude M_L for each intensity class. To ensure equal weight of each intensity class from 1 to 7 inclusive, instrumentally determined local magnitudes were first averaged, giving values 3.4, 3.7, 4.0, 4.5, 4.9, 6.0 and 6.8, respectively. The resulting curve corresponds to $M_L = 0.08{I_0}^2 - 0.04I_0 + 3.41$. This empirical equation was used to determine the magnitudes of historical earthquakes in this study.

A polynomial adjustment (degree 2) results in better regression coefficients, suggesting that the slope increases with magnitude (Figs 8 and 9). To avoid the undesirable weighting effect that favours adjustment with low intensity values (because they are much more numerous than large ones), we determined the average magnitude that corresponds to each intensity represented in the data set, according to the CWB intensity scale (from 0 to 7). As Fig. 9 shows, we obtained average magnitudes 3.4, 3.7, 4.0, 4.5, 4.9, 6.0 and 6.8 for intensities from 1 to 7 (respectively). The best fitting linear relationship did not provide a satisfactory result, but a polynomial function of degree 2 well accounted for the data distribution. We obtained the following empirical relationship between the local magnitude, M_L, and the maximum intensity, I_0:

$$M_L = 0.08I_0^2 - 0.04I_0 + 3.41. \quad (13)$$

This empirical relationship is valid as a first approximation, for intensities 1–7. Earthquakes of inferred intensity 2 or 3 were poorly represented in historical records.

Regarding the largest CWB intensity recorded in Taiwan before the Chi-Chi earthquake was 6. It corresponds to magnitude 6.1 in the above-mentioned empirical relationship. For this reason, adopting the previous CWB intensity scale, earthquakes with magnitude 7 (or higher) would have led to categorize them in magnitude class 6.1 using the empirical relationship in this study. This would not have been reasonable considering such a large difference in magnitude. After the Chi-Chi earthquake the CWB decided to revise the reports for earthquakes with PGA larger than 400 gal, and categorize them in a new intensity class 7 (instead of 6, which now corresponds to no more than 250 gal).

Using our empirical relationship (13), the largest intensity in the currently used CWB intensity scale, 7, corresponds to an average magnitude 7.1. Taking the Chi-Chi earthquake as an example, its recorded local magnitude is 7.3. Considering the recorded intensities and applying the empirical law of Eq. (13), one obtains magnitude 7.1. Since the difference between recorded and calculated local magnitudes is minor for modern, large instrumental earthquakes, the magnitudes actually recorded during the instrumental period were used.

The study of very recent earthquakes since 1995 allows better precision than the empirical relationship (13) permits, especially considering the constraints on focal depth and the distribution of intensities (Fig. 7). Going back in time from the Present to the 20th century, less and less information about earthquakes is available. To ensure homogeneity in our analysis, the empirical relationship (13) was used to evaluate the magnitude of all documented historical earthquakes and maintain consistency with instrumental records. The results from Table 2 and Fig. 8 show that within the range of uncertainties (which are large for most historical earthquakes) there is no need to consider the focal depth, in most cases unknown for ancient earthquakes.

3.5 Comparison with previous studies

Fig. 10 summarizes in a simple way the relationships between our magnitude determinations and those published by Lee (1976), Hsu (1983b) and Tsai (1985). On average, the magnitudes

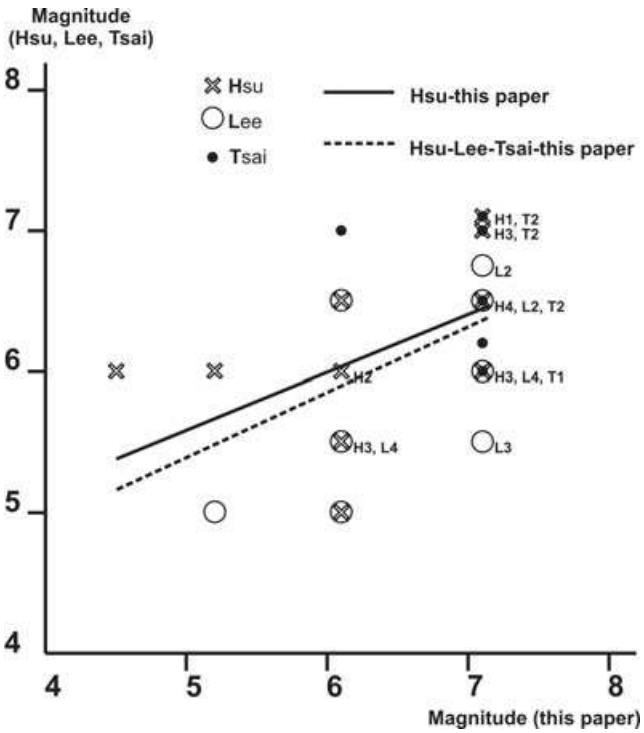

Figure 10. Comparison between magnitudes determined in this study (abscissas) and previous determinations by Lee (1976), Hsu (1983b) and Tsai (1985) (ordinates). Where identical symbols are superimposed, their number is indicated with a letter *L*, *H* or *T* for these three authors, respectively. Two linear regressions have been done, resulting in the black solid line for the comparison between Hsu (1983b) and this paper. The dashed line refers to the comparison between the three authors together and this paper. Separate adjustments for Lee or Tsai are not shown because the number of data and variety in magnitudes were too small to provide significant results.

determined using Eq. (13) are somewhat higher than those indicated by Hsu (1983b) for magnitudes above 6, nearly equal for magnitudes around 6 and slightly lower for magnitudes down to 4.5. Considering the results of these three authors together, the relationship is almost the same. However, because the number of determinations made by other authors is limited and the uncertainties are large for historical earthquakes whatever the magnitude determination method, such correlations should only be regarded as marginally significant.

4 SEISMOGENIC ZONES AND EARTHQUAKE HISTORY

We distinguished five major seismogenic zones in western Taiwan: (I) Taipei-Keelung, (II) Taoyuan-Hsinchu-Miaoli, (III) Taichung-Changhua-Nantou, (IV) Yunlin-Chiayi and (V) Tainan-Kaohsiung-Pingtung (Fig. 11 and Table 3). Although this division is not rigorous, these zones were designed to approximately correspond to major segments of the Taiwan fold-and-thrust belt and its foreland. The size of these zones was chosen according to the accuracy of historical information.

In zone I, fault numbers 1–3 (Fig. 12) were identified but the seismic activity remains low (Fig. 2a) and the historical earthquake records are few. In zone II, a group of fault systems (faults 4–12 in Fig. 12) includes the Shihtan and Shenchoshan Faults responsible for the disastrous 1935 Taichung-Hsinchu earthquake. The Sanyi transfer fault zone (STFZ, Deffontaines *et al.* 1997) approximately corresponds to the boundary between zones II and III. Zone III contains major active fault zones (faults 13–20 in Fig. 12), such as the Chelungpu Fault responsible for the disastrous 1999 Chi-Chi earthquake or the Tuntzuchiao Fault activated by the 1935 Taichung-Hsinchu earthquake mentioned above. In zones III, IV and V, other transfer fault zones were identified (Deffontaines *et al.* 1997), namely the Pakua transfer fault zone (PTFZ, zone III) and the Chiayi transfer fault zone (CTFZ, zone IV) and the Chishan transfer fault zone (ChiTFZ, zone V). Among the faults in zone IV

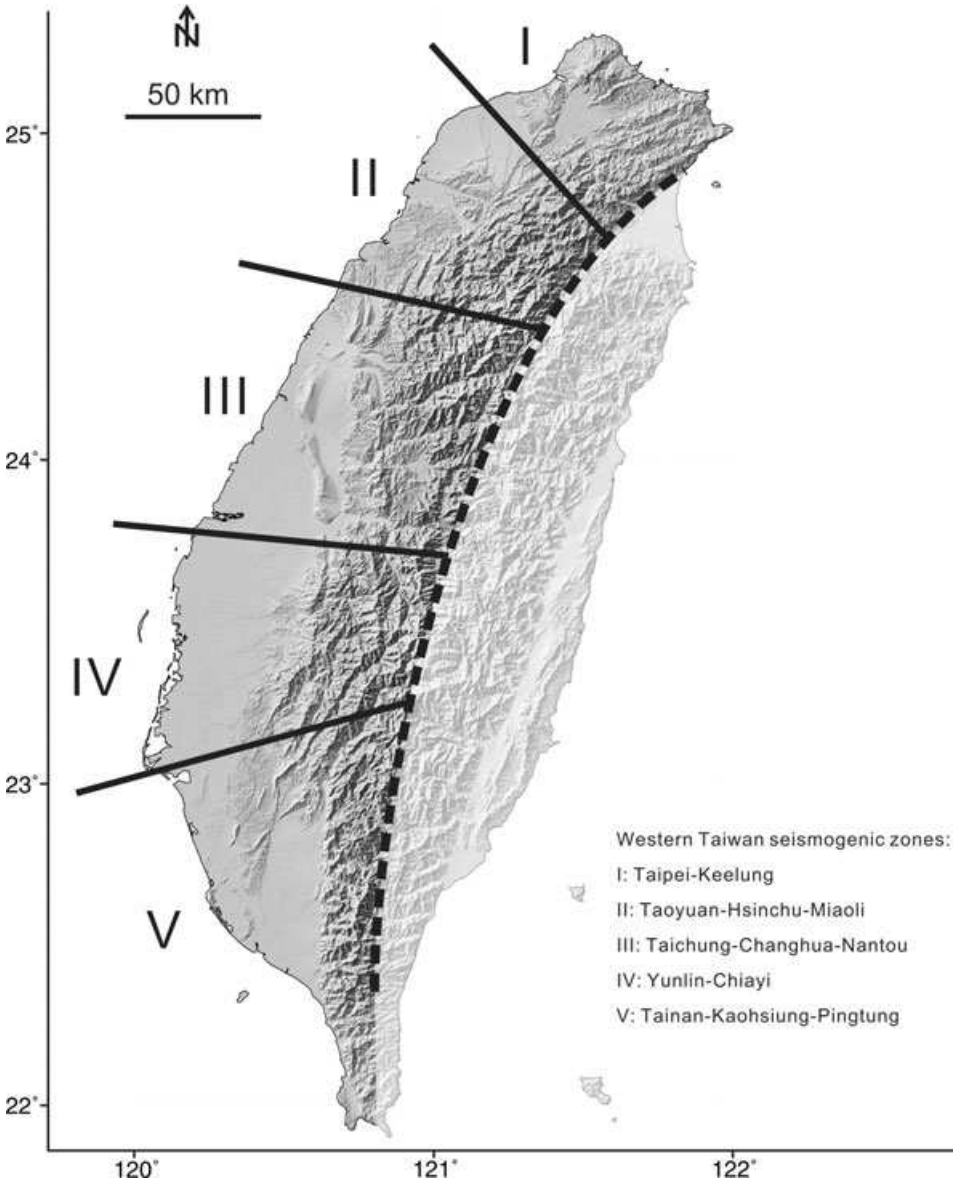

Figure 11. Definition of five seismogenic zones, I–V, in western Taiwan.

Table 3. Summary of historical information about earthquakes of the 17th, 18th and 19th centuries.

Zone	Date	Epicentre	Affected area	Inferred magnitude
V (X)	1624		Tainan	Not applicable
V	1644/07/30	22.80, 120.40	southern Taiwan	6.1 (6) Hsu: 5 (5)
V (X)	1654/12/14	near Anping	southern Taiwan	Assumed: 5.2 (5)
V	1655/01/21	23.00, 120.20	Tainan	6.1 (6) Hsu: 5.5 (5) Lee: 5.5 (7)
unclassified	1658 or 1659		Taiwan	Not applicable
I (X)	1659/10–11 or 1660	near Taipei	Taipei	Assumed: 5.2 (5)
V	1661/01	near Tainan	Tainan	7.1 (7)
V	1661/02/15	23.00, 120.20	Tainan	7.1 (7) Lee: 6 (7.5) Tsai: > = 7
IV	1662/01∼02	near Chiayi	Chiayi	6.1 (6)
V (X)	1676/06/01	near Tainan	Tainan	Assumed: 5.2 (5)
V (X)	Before 1682/08	near Tainan	Tainan	Assumed: 5.2 (5)
V (X)	1682/09	near Kangshan	Kangshan	Assumed: 5.2 (5)
V (X)	1682 (1683)/10/08	Tainan	Tainan	Assumed: 5.2 (5)
IV	1686/05/12	23.50, 120.40	Chiayi, Tainan, Kaohsiung	6.1 (6) Lee: 5.5 (6.5)
I	1694/04∼05	25.00, 121.50	Taipei	7.1 (7) Hsu: 7 (6) Lee: 5.5 (6.5)
V (X)	1705	Tainan	Tainan	Assumed: 5.2 (5)
IV	1711/10/22	23.50, 120.00	Tainan, Chiayi	6.1 (6) Hsu: 5.5 (5) Lee: 6.5 (8) Tsai: 7
IV	1715/10/11	23.50, 120.50	Chiayi	6.1 (6) Hsu: 6.5 (6)
IV	1716/11/02	23.50, 120.50	Chiayi, Tainan, Kaohsiung	4.5 (4) Hsu: 6 (5)
IV (X)	1716/11/04	Chiayi	Chiayi, Tainan, Kaohsiung	Assumed: 5.2 (5)
IV	1717/03/03	23.40,120.40	southern Taiwan	5.2 (5) Hsu: 6 (5)
IV	1720/10/31	23.40, 120.50	Tainan, Chiayi, Kaohsiung	6.1 (6) Hsu: 6 (5)
IV, V (X)	1720		Chiayi-Tainan	Assumed: 5.2 (5)
V	1721/01/05	23.00, 120.30	Chiayi, Tainan, Changhua	7.1 (7) Hsu: 6.5 (6) Lee: 6 (8)
V	1721/09∼10	near Tainan	Tainan	7.1 (7)
V	1722/08/22	near Fongshan	Fongshan, Pingtung	7.1 (7)
V	1723/07/27	near Fongshan	Fongshan	6.1 (6)
unclassified	1730/08/23		Taiwan	Not applicable
III, IV, V (X)	1736/01/29		Tainan, Chiayi, Changhua	Not applicable
IV	1736/01/30	23.10, 120.30, near Chiayi	Chiayi, Tainan, Changhua	7.1 (7) Hsu: 7 (6) Lee: 6 (8) Tsai: 6.5
III, V (X)	1752/07/31		Tainan, Changhua	Assumed: 5.2 (5)
II	1754	Hsinchu	Hsinchu	5.2 (5)
V	1768	near Madou	Tainan	5.2 (5)
III, V (X)	1774/04/26		Tainan, Changhua	Assumed: 5.2 (5)
IV	1776/12	23.50, 120.50	Chiayi	6.1 (6) Lee: 5.5 (7)
IV	1777/11∼12	23.50, 120.50	southern Taiwan	7.1 (7) Hsu: 6 (6) Lee: 5.5
V (X)	1781/04∼06	Kaohsiung	Kaohsiung	Assumed: 5.2 (5)
V	1786/06∼07	Kaohsiung	Kaohsiung	4.5 (4)
IV	1792/08/09	23.60, 120.50, near Yunlin	Chiayi, Changhua, nlin	7.1 (7) Hsu: 7.1 (6) Lee: 6.75 (9) Tsai: 7.1
III, V (X)	1795/01/21 (11/21)		Changhua, Tainan	Assumed: 5.2 (5)
III, V (X)	1795/01/22 (11/22)		Changhua, Tainan	Assumed: 5.2 (5)
V	1797	23.00, 120.20	Tainan	5.2 (5) Lee: 5 (6)
III (X)	1806/03∼04	Changhua	Changhua	Assumed: 5.2 (5)
III (X)	1806/11∼12	Changhua	Changhua	Assumed: 5.2 (5)
III (X)	1809/04∼05	Changhua	Changhua	Assumed: 5.2 (5)
I,II (X)	1810/11∼12		northern Taiwan	Assumed: 5.2 (5)
Unclassified	1811/03/17	23.80, 121.80, east coast	area north of Chiayi	Hsu: 6.5 (6) Lee: 6.5 Tsai: 7.5
Unclassified	1815/07/11	24.70, 121.80, Ilan	Taipei, Ilan	Hsu: 6.5 (6) Lee: 5.5 (7)
Unclassified	1815/10/13∼14	24.00, 121.70, east coast	area north of Chiayi	Hsu: 7.1 (6) Lee: 6.5 (8) Tsai: 7.7
Unclassified	1816/01∼04	24.80, 121.80	Ilan area	Lee: 5.5 (7)
Unclassified	1816/09∼10	24.40, 122.20, northeast coast	Ilan area	Hsu: 7.2 (5)
II	1819/01∼ 1820/02	Miaoli	Miaoli	5.2 (5)
V (X)	1823/02/13	Tainan	Tainan area	Assumed: 5.2 (5)
III	1827/10/05	near Puli	Nantou	5.2 (5)
III (X)	1832/11∼12		Changhua	Assumed: 5.2 (5)
unclassified	1833/12/08	24.60, 122.20, northeast coast	Ilan	Hsu: 7 (5) Lee: 5 (6)
IV	1839/06/27∼28	23.50, 120.50	Chiayi, Tainan	7.1 (7) Hsu: 6.5 (6) Lee: 6.5 (8) Tsai: 6.5
IV	1840/10∼11	23.80, 120.50, near Douliou	Yunlin area	6.1 (6) Hsu: 6 (6) Lee: 5 (6)
III	1842	near Lukang	Changhua	5.2 (5)
III	1845/03/04	24.10, 120.70	Chiayi, Changhua	7.1 (7) Hsu: 6.5 (6) Lee: 6 (8) Tsai: 6
III	1846/08/04	near Changhua	Changhua	4.5 (4)
III	1848/12/03	24.10, 120.50	Tainan, Changhua, Chiayi	7.1 (7) Hsu: 7 (6) Lee: 6.75 (9) Tsai: 7.1
III, IV, V (X)	1848/12/18		Tainan, Changhua, Chiayi	Assumed: 5.2 (5)
III, IV	1849/03/31	Chiayi-Changhua	Hsinchu, Chiayi, Changhua	5.2 (5)
V (X)	1849/05/05	Tainan	Tainan	4.0 (3)

Table 3. (*Continued*.)

Zone	Date	Epicentre	Affected area	Inferred magnitude
V (X)	1849/08/31	Tainan	Tainan	4.0 (3)
V (X)	1849/09/10	Tainan	Tainan	4.0 (3)
V (X)	1849/09/11	Tainan	Tainan	4.0 (3)
IV	1850/04∼05	23.50, 120.40	Chiayi	6.1 (6) Hsu: 5.5 (5)
III	1851/04/09		Changhua	4.5 (4)
V (X)	1851/04/12	Tainan	Tainan	4.0 (3)
V (X)	1851/04/14	Tainan	Tainan	4.0 (3)
V (X)	1851/04/15	Tainan	Tainan	4.0 (3)
I (X)	1853/05∼08	near Tatunshan	Tatunshan	Assumed: 5.2 (5)
I, II	1860/11∼12		Taipei, Hsinchu, Miaoli	5.2 (5)
I, II (X)	1862/01∼04		Taipei, Hsinchu, Miaoli	Assumed: 5.2 (5)
IV, V (X)	1862/06/05		Tainan, Chiayi, Changhua	Not applicable
IV	1862/06/07	23.20, 120.20	Tainan, Chiayi, Changhua	7.1 (7) Hsu: 6.5 (6) Lee:6.5 (8) Tsai: 7
I, II (X)	1862/11∼12		Taipei, Hsinchu, Miaoli	Assumed: 5.2 (5)
I	1865/11/06	24.90, 121.60	Taipei, Keelung	7.1 (7) Hsu: 6 (6)
I, II (X)	1866/02∼03		Taipei, Hsinchu, Miaoli	Assumed: 5.2 (5)
V	1866/12/16		Kaohsiung	5.2 (5)
Unclassified	1867/12/18	25.30, 121.70, offshore	Taipei, Keelung, Hsinchu	Hsu: 7 (6) Lee: 6 Tsai: 7
V	1870	22.40, 120.60	Pingtung	6.1 (6) Lee: 5.5 (7)
V	1873	Tainan	Tainan	5.2 (5)
II	1880/02/29	Miaoli	Miaoli	6.1 (6)
V	1880/06∼07	Tainan	Tainan	5.2 (5)
I	1880/07/20	Taipei	Taipei	4.5 (4)
II	1881/02/18	24.60, 120.70	Taipei, Hsinchu, Miaoli	7.1 (7) Hsu: 6 (6) Lee: 5.5 (7) Tsai: 6.2
IV, V (X)	1881/06/16		Tainan, Chiayi	Assumed: 5.2 (5)
Unclassified	1881/06/17		Hualien	Not applicable
I	1881/07/06		Keelung	4.0 (3)
I	1881/12/08	near Taipei	Taipei	5.2 (5)
IV, V (X)	1882/05/27		southern Taiwan	Assumed: 5.2 (5)
II (X)	1882/08∼09	near Hsinchu	Hsinchu	Assumed: 5.2 (5)
Unclassified	1882/12/09	23.00, 121.40, offshore	Entire island of Taiwan	Hsu: 7.5 (5) Lee: 6.25 (7.5) Tsai: 7.5
IV	1884/01	near Chiayi	Yunlin, Chiayi	6.1 (6)
IV	1885/05∼06	near Chiayi	Yunlin, Chiayi	6.1 (6)
II (X)	1887/11∼1888/02	near Miaoli	Miaoli	Assumed: 5.2 (5)
Unclassified	1889/10/29			Not applicable
Unclassified	1889/11/21		Taiwan	Not applicable
Unclassified	1890/3/16		Taiwan	Not applicable
Unclassified	1890/05/04		Taiwan	Not applicable
Unclassified	1892/02		Taiwan	Not applicable
V (X)	1892/04/02	near Tainan	Tainan	Assumed: 5.2 (5)
V	1892/04/22	Tainan	Entire island of Taiwan	5.2 (5)
Unclassified	1892/06/11		Taiwan	Not applicable
Unclassified	1892/07/20		Taiwan	Not applicable
Unclassified	1892/08/21		Taiwan	Not applicable
V (X)	1892/09		Tainan	Assumed: 5.2 (5)
V (X)	1892/12		Tainan	Assumed: 5.2 (5)
V (X)	1893/01		Tainan	Assumed: 5.2 (5)
V (X)	1893/04		Tainan	Assumed: 5.2 (5)
V (X)	1893/05		Tainan	Assumed: 5.2 (5)
V (X)	1893/06		Tainan	Assumed: 5.2 (5)
Unclassified	1893/07/15		Taiwan	Not applicable
Unclassified	1893/08/24		Taitung	Not applicable
I	1893/10/17	near Taipei	Taipei	5.2 (5)
V (X)	1893/10		Tainan	Assumed: 5.2 (5)
I	1893/11/14	Taipei	Taipei	4.0 (3)
Unclassified	1894/02/12		Taitung	Not applicable
Unclassified	1894/03/09		Taitung	Not applicable

(faults 21–26 in Fig. 12), the most active are the Meishan Fault (fault 22 in Fig. 12) re-activated by the 1906 Meishan earthquake (Omori 1907a,b; Bonilla 1975) and the Chukou Fault. In zone V, other active faults, certain or suspected, exist (faults 27–35 in Fig. 12), in addition to some transfer fault zones such as the Chishan transfer fault zone (ChiTFZ) and the Fengshan and Kaohsiung transfer fault zones. The Hsinhua Fault (27 in Fig. 12) was responsible for the 1946 Hsinhua earthquake (Bonilla 1975).

Table 3. (*Continued*.)

Zone	Date	Epicentre	Affected area	Inferred magnitude
V (X)	1894/09		Tainan	Assumed: 5.2 (5)
V (X)	1894/11		Tainan	Assumed: 5.2 (5)
V (X)	1895/01	near Tainan	Tainan	Assumed: 5.2 (5)
V (X)	1895/04	near Tainan	Tainan	Assumed: 5.2 (5)
V (X)	1895/06	near Tainan	Tainan	Assumed: 5.2 (5)
Unclassified	1896/02/12		Ilan	Not applicable
Unclassified	1897/03/15	near Ilan	Ilan, Taipei	Not applicable

Data compiled from five sources: CWB website (http://www.cwb.gov.tw/), Hsu (1983a), Lee *et al.* (1976), Hsu (1983b) and Tsai (1985). Explanation of columns as follows:
First column: five Roman numerals I–V refer to the seismogenic zones of western Taiwan located in Fig. 11: Taipei-Keelung (Zone I), Taoyuan-Hsinchu-Miaoli (Zone II), Taichung-Hsinchu-Miaoli (Zone III), Yunlin-Chiayi (Zone IV) and Tainan-Kaohsiung-Pingtung (Zone V). For those historical events that could not be categorized into these five above-mentioned zones, 'unclassified' was assigned. Symbol 'X' indicates earthquakes that could be categorized but with intensity that could not be evaluated using the CWB intensity scale.
Second column: Date of earthquake occurrence. Values in brackets indicate another possible date according to other sources.
Third column: Preferred location of epicentre (latitude and longitude in degrees, and/or city or area) of historical earthquakes.
Fourth column: Affected regions.
Fifth column: Inferred magnitudes, as determined using the average empirical relationship between M_L, local magnitude, and I_0, epicentral intensity: $M_L = 0.08{I_0}^2 - 0.04I_0 + 3.41$ (Eq. 13 and Fig. 9). Values between parentheses after inferred magnitudes are the estimated intensities. When magnitude could not be determined, magnitude 5.2 and intensity 5 were assumed (explanation in text). Earthquakes that could not be used in the study correspond to mention 'Not applicable'. Previous estimates from other authors indicated with author's name first, estimated magnitude and given intensity (between parentheses).

4.1 Main historical earthquakes of the West Taiwan belt

Before considering the extensive records of seismic activity during the last 3–4 centuries, it is appropriate to consider the most notorious destructive earthquakes that occurred in the different segments of western Taiwan, as defined in Fig. 11.

Zone I (Taipei segment, northern Taiwan): a major earthquake took place in 1694 (April 24–May 23), during the 33rd year of Kangxi's reign (Ching Dynasty). A part of the Taipei Basin subsided and water intruded the Basin, forming the Kangxi Taipei Lake, as noted from an archaeological excavation report of the Taipei County. The estimated intensity was 6–7 (Table 3). Although Lee *et al.* (1976) provided a lower value, our determination supports Hsu's (1983b) conclusion regarding the magnitude, that is, 7 or 7.1.

Severe earthquakes once again occurred in zone I in 1865, 1866 and 1867. The November 6, 1865 earthquake produced extensive damage. In Taipei, Keelung and other northern areas, there were quite a number of deaths. The best-built Chinese houses collapsed; all houses near Kimpauli collapsed and fell into the sea. According to quotation from Father P.F. Da Sylva in Kaohsiung (at the opposite tip of the island), several earthquakes, especially as series in mid-November, the first strike was on November 6. Our estimated magnitude is 7.1 (with intensity 7), larger than Hsu's (1983b) value, 6.

The most recent major earthquake in this northern zone occurred on April 15, 1909, as the Taipei earthquake (Fig. 3). The instrumentally recorded magnitude was 7.3, which does not imply intensity 7 according to Eq. (13) calibrated for shallow earthquakes but probably lower intensity, because the focal depth was about 80 km, that of an intermediate-focus earthquake. This explains why despite large magnitude only 9 people died and 122 houses were totally destroyed.

Zone II (Taoyuan-Hsinchu-Miaoli segment): a February 18, 1881 destructive earthquake, with 210 collapsed houses and 11 casualties reported (according to information displayed on the CWB Website), had intensity 6–7 an estimated magnitude ranging from 5.5 (Lee *et al.* 1976) to 7.1 (Table 3).

Later, the April 21, 1935 Taichung-Hsinchu earthquake (recorded magnitude $M_L = 7.1$) caused the largest casualties in the 20th century in Taiwan, as mentioned earlier. It thus deserves classification as intensity 7 earthquake according to eq. (13). The main shock was located near Miaoli, but several large aftershocks occurred over a large area including not only zone II (with two shocks in May and July 1935, killing 44 persons and totally destroying 1,762 houses) but also zone III (with two shocks in May and June, totally destroying 7 houses).

Zone III (Taichung-Changhua-Nantou segment): on March 4, 1845 a major earthquake occurred in the Taichung basin area, affecting the region of Changhua and even Chiayi (in zone IV), with 381 persons killed and 4,220 houses collapsed. As for some earthquakes mentioned above, we calculated a magnitude, 7.1, larger than those previously proposed (6 or 6.5: Lee *et al.* 1976; Hsu 1983b and Tsai 1985; Fig. 10).

On December 3, 1848, another major destructive earthquake struck the same area, with 1,030 persons killed and 13,993 houses collapsed. Magnitudes estimates provide values in the range 6.75–7.1. Several earthquakes occurred at the beginning of the 20th century, especially in 1909 and 1916–1917, most of them with moderate magnitudes (6 on average) but shallow depths accounting for significant damage (71 killed, 1,038 houses totally destroyed).

The largest earthquake in zone III was the September 21, 1999, Chi-Chi earthquake ($M_L = 7.3$) causing the casualties already mentioned. This largest instrumentally recorded earthquake on the Taiwan Island (magnitudes 8 have been recorded offshore, east and northeast of Taiwan) was followed by large series of aftershocks during about 1 yr. The depth was shallow, about 8 km according to CWB website, consistent with measured intensity 7.

Zone IV (Yunlin-Chiayi segment): on January 30, 1736, a big earthquake struck the Chaiyi-Tainan area, causing 372 deaths, 129 injured and 698 houses damaged. Magnitude estimates ranges from 6–7.1; our estimate, 7.1, is close to Hsu's, 7 (1983b).

On August 9, 1792, another major earthquake occurred in the Yunlin region. It affected a large area (Changhua, Yunlin and Chiayi). 617 people were killed with 781 injured and 24,621 houses were damaged. The four magnitude estimates are compatible, 6.75 (Lee *et al.* 1976) or 7.1 (Hsu 1983b; Tsai 1985 and this paper).

In a destructive earthquake near Chiayi on June 27, 1839, 117 people were killed and 534 injured along with 7515 houses

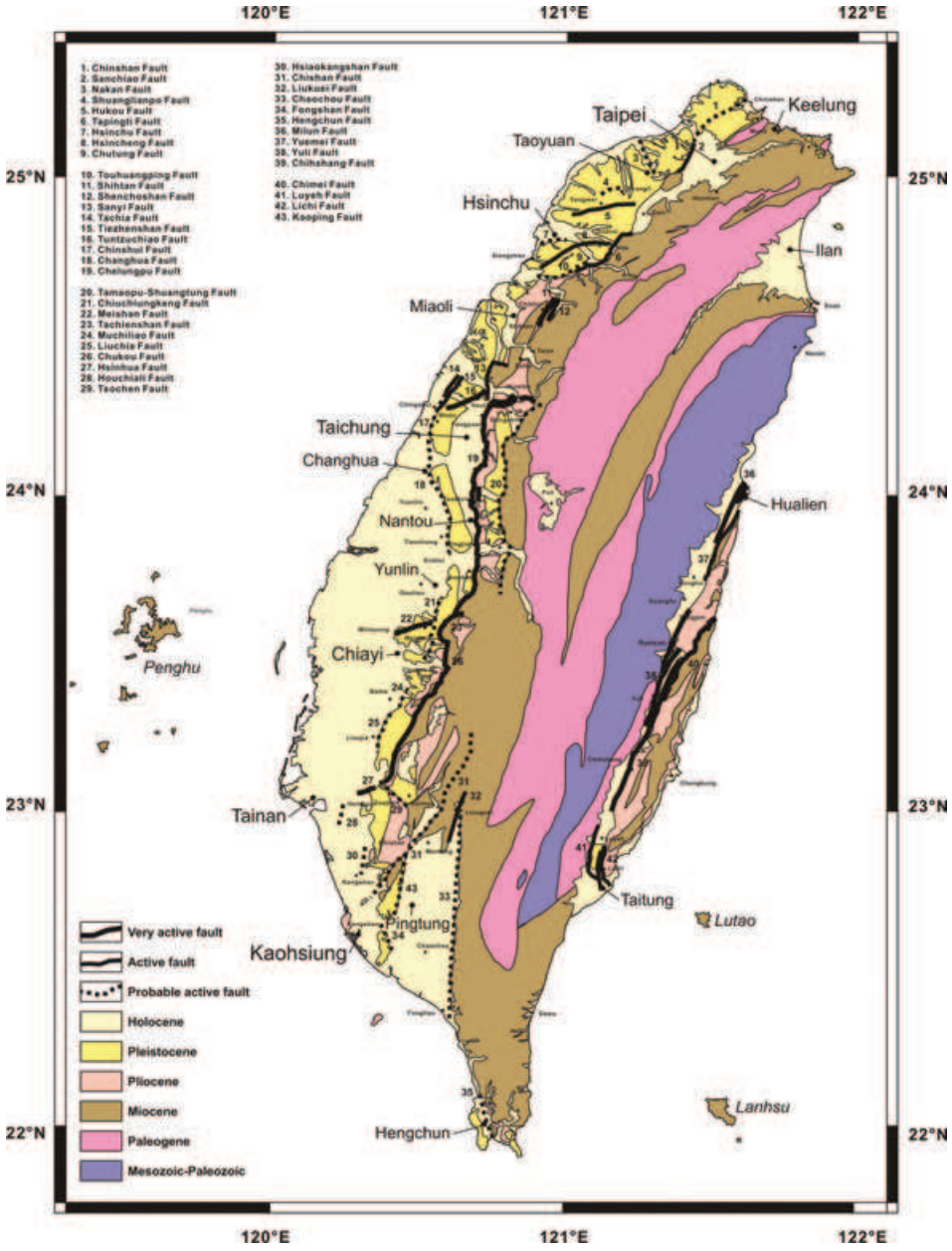

Figure 12. Map of active faults in Taiwan (adapted from Central Geological Survey, MOEA 2005).

collapsed. Our magnitude estimate is 7.1, higher than those of the three other authors (6.5).

More than 500 people died and more than 500 houses collapsed on June 7, 1862 earthquake. This event affected Changhua, Chiayi and Tainan. Estimated magnitudes range from 6.5 (Lee *et al.* 1976; Hsu 1983b) to 7.1 (this paper). Tsai (1985) provided an estimated magnitude 7, close to ours.

During the instrumental period, the March 17, 1906 Meishan earthquake ($M_L = 7.1$) produced a 13 km long rupture trace, activating the right-lateral Meishan Fault. Detailed reports and map exist concerning this earthquake (Omori 1907a,b). This Meishan earthquake killed 1,258 people and 6,769 houses totally destroyed. Large damage resulted from shallow focal depth, 6 km. Four destructive aftershocks in the same area (March 26, April 4, 7 and 14, with a total of 17 deaths and 1,891 totally destroyed houses) had magnitudes ranging from 4.9 to 6.6. Despite these limited magnitudes, high damage also resulted from shallow focal depths, 5–20 km.

The most recent major destructive earthquake in this zone was the December 17, 1941 Chungpu earthquake ($M_L = 7.1$), causing 358 deaths and total destruction of 4,520 houses. As before, the shallow focal depth, 12 km, resulted in large damage.

Zone V (Tainan-Kaohsiung-Pingtung): on January 21, 1655, an earthquake struck the Tainan region. City walls cracked and felt aftershocks lasted for about three weeks. Hsu (1983b) and Lee *et al.* (1976) provided identical magnitude estimates, 5.5, lower than ours, 6.1.

A severe earthquake happened on February 15, 1661, causing 27 houses collapsed in Tainan. Felt aftershocks lasted for six days. Whereas Lee *et al.* (1976) provided a low estimated magnitude, 6, we determined a value, 7.1, consistent with Tsai's (1985) determination (7 or larger).

Earthquakes occurred in 1721, with one shock on January 5 and a poorly documented one in September–October, damaging and tilting houses and temples and killing 'many people'. Magnitude estimates range from 6 (Lee *et al.* 1976) to 7.1 (this paper). Earthquakes near Fongshan, causing eruptions of mud volcano, were reported during the following 2 yr but information is scarce.

4.2 Techniques used to summarize historical earthquake activity

In this paper, the magnitude estimates of the earthquakes predating the instrumental period have been done according to Eq. (13) and Fig. 9, based on consideration of both the maximum intensity (Fig. 5) and the limited effect of depth (Fig. 8) in the 0–40 km range documented from instrumentally recorded earthquakes. Knowing that large uncertainties exist, three different types of illustration are adopted to present the results. In all diagrams, the axis of abscissas shows the time, from year 1600 to 2008.

The first type of diagram involves a non-cumulative representation of earthquake magnitude as ordinates (Figs 13a, 14a and 15a). Each historical earthquake is represented by a bar with uniform thickness and variable height indicating magnitude. For successive earthquakes, the bar height indicates the largest magnitude and the number of earthquakes is indicated on top of the bar. For some earthquakes, the magnitude could be calculated (black bars in diagrams), whereas for others this determination could not be made so that a value of 5.2 was assumed (grey bars in diagrams). This value was obtained based on the assumption that intensities smaller than 5 (0–4 in CWB intensity scale) in earthquakes would not, in general, produce significant damage. Applying intensity 5 as the minimum intensity of reported historical earthquakes and using our empirical relationship (13), one obtains magnitude 5.2.

The other two types of diagrams in Figs 13, 14 and 15 involve a cumulative representation of the earthquake energy or the elastic strain release. Regarding the seismic moment plots (Figs 13b, 14b and 15b), the energy is simply calculated as a function of the magnitude, according to Eqs 12 and 13 and using the same assumptions as above. Introducing or not the earthquakes with assumed magnitude 5.2 did not significantly modify the result (compare solid and dashed lines in Figs 13b, 14b and 15b). Not surprisingly, the reconstructed energy distribution through time is mainly controlled by the large magnitudes.

In the last diagram (Figs. 13c, 14c and 15c), the seismic strain release is plotted, following an approach already adopted in Iceland by Stefánsson and Halldórsson (1988). The determination of the seismic strain release is based on a previous work by Benioff (1951), who demonstrated that the release of the elastic strain related to an earthquake is proportional to the square root of the dissipated energy. Therefore, in the seismic strain release plot, the energy is calculated as a function of the square root of the seismic moment magnitude.

Regardless of scale the cumulative curves obtained by plotting the seismic moment and its square root significantly differ although the information used is the same (compare b and c in Figs 13, 14 and 15). As an example, the cumulative strain release plot of zone III, the Taichung-Changhua-Nantou belt segment (Fig. 13c), reveals three major steps of similar amplitudes in 1850, 1920 and 1999. In the corresponding plot of seismic moment (Fig. 13b) the 1999 step is higher than the other two steps together. This difference is a direct effect of the Benioff's relationship. If for instance the sum of the strain release for two identical earthquakes equals that

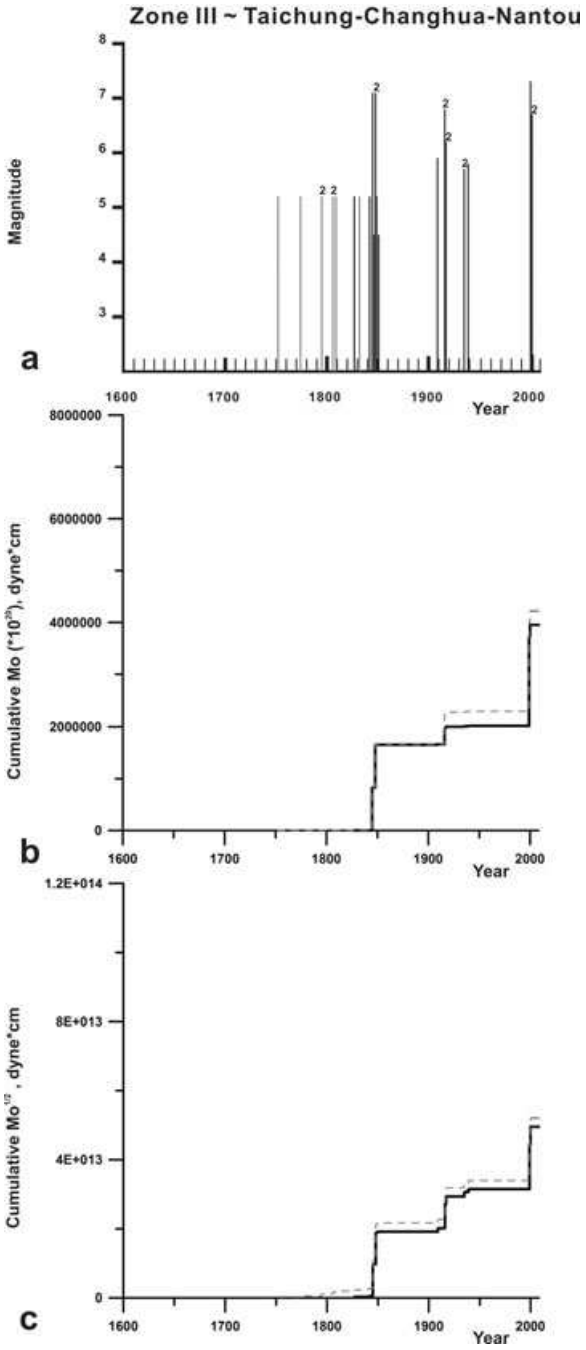

Figure 13. Occurrence of historical earthquakes and inferred time distribution of elastic energy and strain. Example of zone III (Taichung–Changhua–Nantou, location in Fig. 11). In all diagrams, the axis of abscissas shows time, from year 1600 to year 2008. (a) Non-cumulative representation of major earthquakes, with earthquake magnitude as ordinate. Each historical earthquake is represented by a bar of uniform thickness and height indicating magnitude; when two (or more) earthquakes occurred the same year, the bar height indicates the largest magnitude and the number of earthquakes is indicated on top of bar. Black bars refer to determined magnitudes, grey bars refer to unknown magnitudes (in this case a value of 5.2 was assumed, see text). (b) cumulative energy release calculated as a function of the magnitude, according to Eqs 12 and 13 and using the same assumptions as above (solid line for earthquakes with estimated magnitude, dashed line for both estimated and assumed magnitudes). (c) cumulative seismic strain release, as determined based on the Benioff's law (1951) indicating that the release of the elastic strain related to an earthquake is proportional to the square root of the dissipated energy.

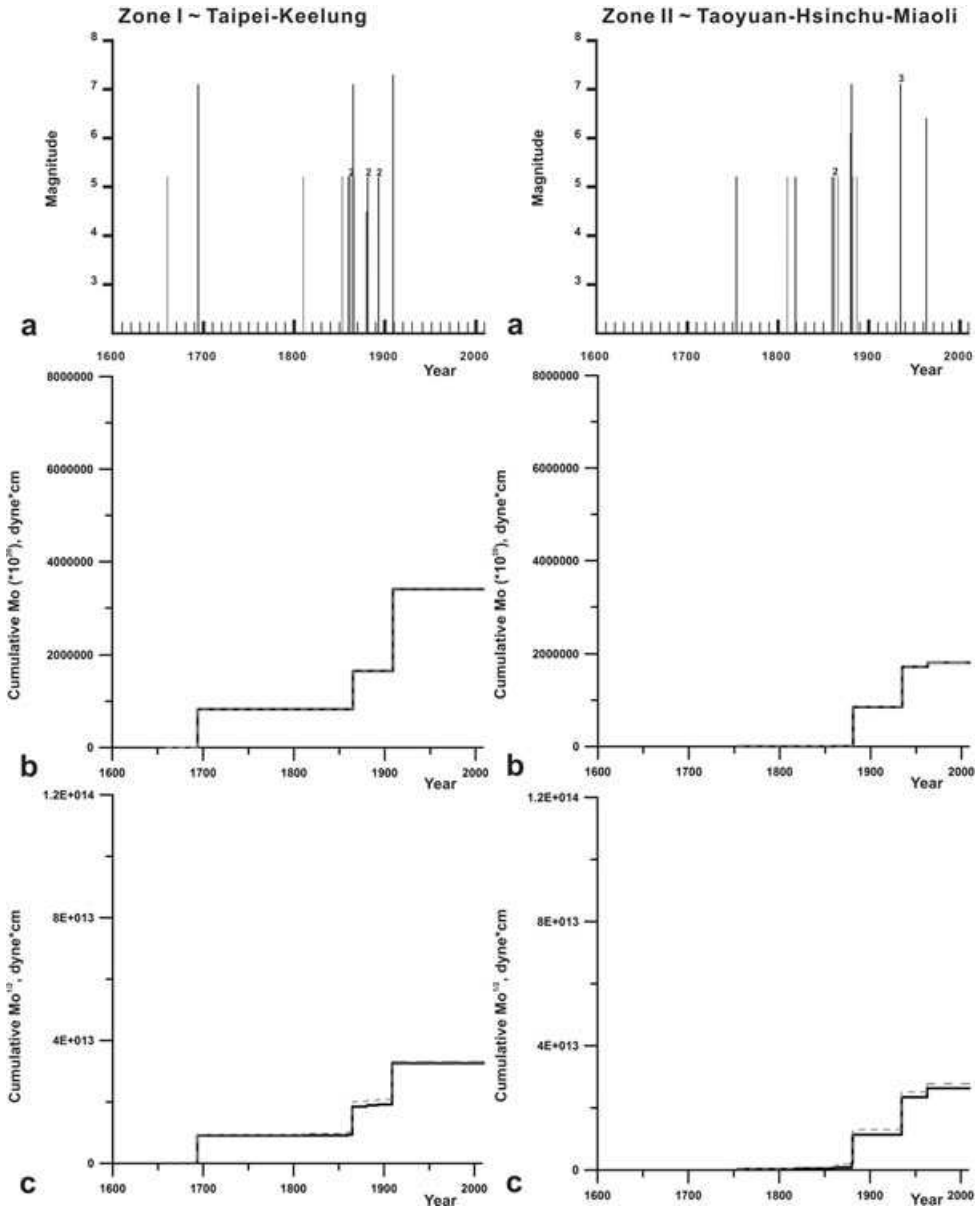

Figure 14. Results for zones I and II (location in Fig. 11). Same caption as for Fig. 13.

of a single larger earthquake, the seismic moment of the latter is twice that of the two smaller earthquakes together. Conversely, if the seismic moment of the large earthquake equals the sum of the seismic moments of the smaller two earthquakes, its strain release is only 70% of that of these two earthquakes together. Both types of curves are shown in the figures, because their comparison allows one to better delineate the major historical events (such as for the 1850 and 1920 events in Fig. 13).

In terms of physical meaning, the curve of cumulative strain release better reveals earthquakes occurring at short time intervals, whereas the curve of cumulative seismic moment rather highlights large isolated earthquakes (such as for the 1999 Chi-Chi earthquake). The cumulative strain release plot better reflects the number of earthquakes—indeed an important parameter during a seismic sequence—whereas the cumulative seismic moment curve directly reflects the amount of energy released.

The earthquake history of each zone is thus summarized in Figs 13–15. In Zones I, II, III, IV and V, respectively, the numbers of historical seismic events used to plot the curves are 7, 9, 18, 35 and 17 for estimated magnitudes only (solid curves), and 15, 15, 27, 39 and 52 when all events, including assumed magnitudes 5.2, are considered.

5 DISCUSSION AND CONCLUSION

In zone I (Taipei-Keelung), few earthquakes before 1850 could be studied. More historical records could be found from 1850 to 1910. Later, the area remained seismically relatively quiet until now. Despite the lack of ancient documents, the diagrams on the left side of Fig. 14 suggest that the earthquake cycle of Taipei-Keelung region is longer than a century; it may be as long as about 160 yr. The 1909 Taipei ($M_L = 7.3$) earthquake was the latest destructive earthquake in this zone. This is consistent with the general opinion that in the Taipei-Keelung area the strain accumulation and release is by Taiwan standards a relatively slow process.

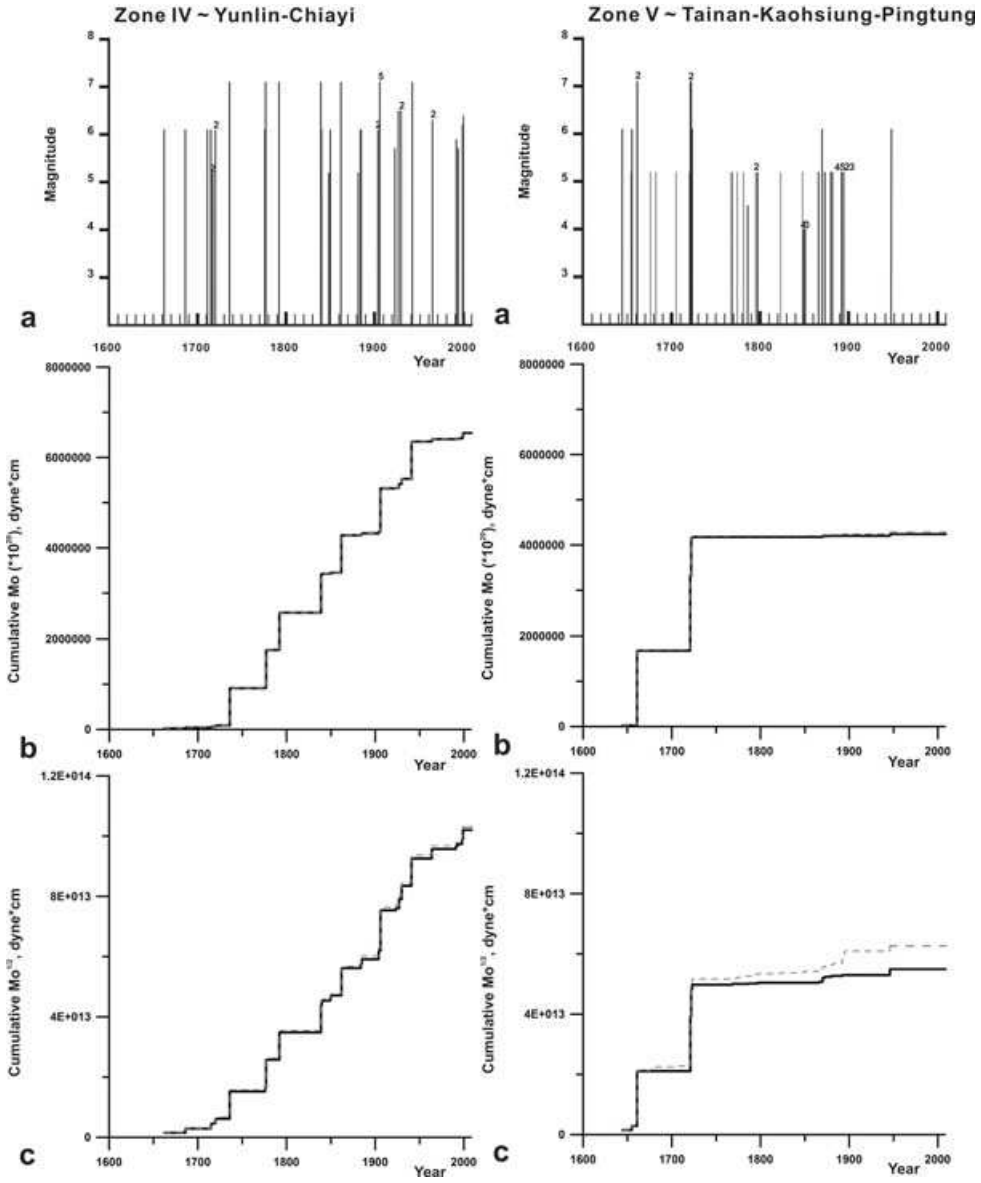

Figure 15. Results for zones IV and V (location in Fig. 11). Same caption as for Fig. 13.

Despite the lack of reliable information before 1750 (the Chinese settlement in and around Hsinchu started in the late 17th century), the diagrams on the right side of Fig. 14 may suggest a 50–60-year earthquake cycle in zone II (Taoyuan-Hsinchu-Miaoli), mainly based on four major events between 1754 and 1935. However, after the 1935 Taichung-Hsinchu earthquakes, with the main shock ($M_L = 7.1$) and two aftershocks in Fig. 14a (right side), no very large event was recorded until now. Considering the existence of at least four regularly spaced major events in the 18th, 19th and 20th centuries, this absence of important event since at least 73 yr should not be interpreted as evidence of seismic quietness, but rather indicates strain deficit and suggests continuing accumulation of elastic stress. Independent analyses of geodetic, GPS data predating the 1999 Chi-Chi earthquake of zone III revealed an excess of compressive strain across the Taiwan belt in zone II (Chang *et al.* 2003), which supports our hypothesis of compressive elastic stress accumulating since 1935.

The records in zone III (Taichung-Changhua-Nantou) reveal higher levels of seismic activity; it is the second most important zone in western Taiwan in terms of total strain release. Three major seismic events took place in 1845–1848, 1909–1917 (including 1916–1917 Nantou earthquake series) and 1999 (Chi-Chi earthquake, $M_L = 7.3$, Fig. 3). This succession may suggest a 70–80 year earthquake cycle (Fig. 13a). As mentioned before, the relative importance of the earthquakes of the early 20th century depends on whether one considers the cumulative energy (Fig. 13b) or the cumulative strain release (Fig. 13c). Taking the energy in sole account, one would retain duration of about 1.5 century for the seismic cycle. However, the oldest records mention several events between 1750 and 1850. The lack of earlier information is not surprising because Taichung was founded in the early-middle 18th century.

Throughout the last four hundred centuries, the seismic activity in zone IV (Yunlin-Chiayi) resulted in frequent destructive earthquakes (Fig. 15a, left side). As Chiayi was founded in the early-middle 17th century, relatively old records are available. Because of the high earthquake frequency, the cumulative curves show a staircase aspect for both the energy and strain release (Figs 15b and c, respectively, left side). As a consequence, it is not easy to determine

the major trends of the earthquake history for this zone. A possible earthquake cycle of about 35–50 yr is considered, based on consideration of 5–7 major events since 1750. Not surprisingly, this region is the highest cumulative strain release zone among the five zones of Fig. 11. The major 1906 Meishan ($M_L = 7.1$) and 1941 Chungpu ($M_L = 7.1$) earthquakes struck this zone. The highest number, 5 on the top of bar in Fig. 15a (left) refers to the 1906 main shock and the four aftershocks of the Meishan earthquakes.

Finally, although destructive earthquakes took place in zone V (Tainan-Kaohsiung-Pingtung), there is no reliable indication of earthquake cycle from our records (Fig. 15, right side). Good ancient records are available in this region (as well as in zone IV) because Tainan, founded in the early 17th century, was the early capital of the Taiwan Island. Five or six seismic events took place between 1650 and 1950, but this does not support any conclusion regarding a time spacing of 60–75 yr because time intervals are irregular (Fig. 15a, right side). Despite significant earlier activity no major earthquake has occurred there since about 50 yr, the last destructive earthquake being the 1946 Hsinhua earthquake, $M_L = 6.1$. Quite significant aseismic deformation also occurs in this area (e.g., the Tainan Tableland), probably resulting in a complex balance of energy dissipation.

The seismic activity recorded on land during the instrumental period remained generally low in zone V. Two large earthquakes recently occurred offshore Hengchun on December 26, 2006, with magnitudes 7.0 (Fig. 3), at large crustal depths. These earthquakes are not considered herein because they originated from a subduction-related context that does not reflect the usual seismotectonic activity on land at the front of the advancing Taiwan fold-and-thrust belt. Remarkably, low levels of release in elastic energy and strain release prevailed since nearly three centuries (Figs 15a and b, right side). To these respects, and considering the ancient earthquakes of 1655–1661 and 1721, this southern area should not be regarded as seismically quiet or free of elastic strain accumulation.

In this study, we aimed at providing a consistent picture of the earthquake history since the 17th century in western Taiwan, with new insights in terms of the earthquake cycle. Several difficulties arose. Whereas the instrumental period (since 1900) and even the 19th century provided systematic account of major earthquakes, the records of the previous centuries were generally inaccurate and often incomplete. It was consequently necessary to harmonize quite different sources of information. Had this process been absent, the apparent earthquake activity would have increased with time, which in fact is a mere effect of the improvement in density and accuracy of information. To this respect, it is worth noting that many major earthquakes of the 17th and 18th centuries are poorly known, improperly located on even ignored. Also, the qualitative description of the earthquake damage, which our magnitude estimates were issued from regarding ancient earthquakes, was highly dependent on the capacity and interest of the recording persons, and hence cannot be considered homogeneous. It was also influenced by the evolving density of the population and city growth at various places since the Chinese settlement that massively started during the 17th century.

In contrast, the modern seismological networks, especially since 1992, are dense enough to provide a picture that can be regarded homogeneous, at least for earthquakes of magnitude 2–3 and higher. Another major difficulty in this study was the absence of any quantification of magnitudes from original records. Following other researchers (Lee *et al.* 1976, Hsu 1983b and Tsai 1985), we consequently evaluated the magnitudes of the ancient earthquakes based on consideration of maximum intensities, which themselves were inferred from damage records. We took advantage of the existence of systematic determinations of magnitudes, depths and intensities for recent earthquakes, such as in the CWB database (Shin *et al.* 1996 and Wu *et al.* 1997) to carry out a calibration of magnitudes-intensity relationships (Fig. 8), which in turn was applied to ancient earthquakes through the use of the derived empirical law (eq. 13 and Fig. 9). This aspect, however, required careful consideration of the magnitude definitions and intensity scales, which changed through time. We obtained estimated magnitudes for many historical earthquakes, resulting in a certainly imperfect but technically homogeneous list (Table 3). For the largest earthquakes already considered by other authors (Fig. 10), we obtained magnitude values in many cases close to those given by Tsai (1985) but significantly higher than those published by Hsu (1983b) and especially Lee *et al.* (1976). For many historical earthquakes it was however impossible to evaluate the magnitude, so that as a major limitation we had to consider a reasonable minimum value, 5.2. This value was chosen based on a comparison with the present-day instrumental data, suggesting that shallow earthquakes with magnitudes larger than 5 are commonly felt in a way that justifies written records, as was done in the past.

The final step consisted of building graphs that describe in a synthetic way the seismic activity of the last four centuries in terms of seismic events, cumulative seismic energy and cumulative strain release. New difficulties arose, especially dealing with the delineation, in western Taiwan, of regions that were large enough to compensate the effect of very large location uncertainties for ancient earthquakes, but small enough to correspond to relatively homogeneous domains in terms of geological structure and seismogenic major units. We finally selected five major segments of the western Taiwan belt, as described in Fig. 11. The corresponding graphs were used to evaluate the duration of the average seismic cycle in these regions (Figs 13–15). Although the total period considered (less than 400 yr) is too short to allow accurate determinations of seismic cycle, this synthesis provides some insights and guidelines. It appears that the different regions exhibit contrasting behaviours in terms of both the importance and frequency of destructive earthquakes.

In northernmost Taiwan, near Taipei (Zone I), the long cycle, possibly 160 yr, reveals slow processes of elastic strain accumulation, which well fits with both the low strain values revealed by geodetic analyses and the relatively low geological activity of the northernmost segment of the Taiwan collision belt. As a consequence, Zone I may be regarded as relatively quiet in terms of seismic hazard, provided that the estimated length of the seismic cycle, 160 yr, is correct. This is because the last very large event (recorded magnitude 7.3) has occurred in 1909, about 100 yr ago.

In central West Taiwan, near Taichung (Zone III), large earthquakes have repeatedly occurred at time intervals that may average 150 yr (considering a high threshold level of magnitude-intensity) or 70–80 yr (adopting a lower level). Because the last major earthquake, Chi-Chi ($M_L = 7.3$), has occurred in 1999, the corresponding area is thus regarded as being now in the early inter-seismic stage.

In southern Taiwan, near Kaohsiung (zone V), the picture is more confuse, probably because of high geological and seismotectonic diversity near the transition from the Taiwan collision to the Manila Trench subduction zone. However, consideration of ancient destructive events suggests that strain accumulation occurs along several apparently locked major faults, such as the Chaochou Fault.

Although there is a major contrast in seismic activity between zone III of Central Taiwan on one hand and the northern and southern tips of the Island on the other hand, zones I and V should by no means be regarded as equivalent. Active deformation is much larger

to the South, as shown by GPS studies suggesting that the Chaochou Fault is locked rather than inactive and revealing large deformation in the southwest Pingtung Plain (Hu *et al.* 2007). Although no large destructive earthquake has been recorded along this major fault zone during the last four centuries, the morphological expression reveals high tectonic activity during the late Quaternary, suggesting together with present-day deformation measurements that despite a relative mechanical weakness of the crust high amounts of elastic energy probably accumulate in this area. Thus the threat of the high-angle Chaochou Fault cannot be ignored while evaluating the seismic hazard in southern Taiwan.

Between central Taiwan (zone III) and these northern and southern regions (zones I and V, respectively), major earthquakes frequently occurred in the past in two intermediate regions (zone II for Taoyuan-Hsinchu-Miaoli and zone IV for Yunlin-Chiayi). As a consequence of this general distribution, the intermediate areas between Central Taiwan and the northern and southern zones deserve particular attention. South of Taichung, in the Chiayi area (zone IV), a possible seismic cycle of 30–50 yr on average can be considered, with the 1941 Chungpu earthquake ($M_L = 7.1$) as the last major destructive event. North of Taichung, in the Hsinchu-Miaoli area (zone II), the historical data suggest that the most probable duration of the average seismic cycle is 50–60 yr. However, the most recent large earthquakes occurred in 1935, as the Taichung-Hsinchu earthquakes ($M_L = 7.1$). The present-day situation seems to be beyond reasonable bounds of the earthquake cycle, with 67 (zone IV) and 73 yr (zone II) elapsed since the last very large earthquakes. Both these zones II and IV are thus probably subject to elastic strain accumulation, and hence a deficit in strain release.

Despite the uncertainties related to major earthquake-related deformation, and hence to the seismic cycle, the analyses of the present-day deformation of Taiwan, based on GPS results (e.g. Yu and Chen 1994; Yu *et al.* 1997, 1999; Hu *et al.* 2001, 2007; Chang *et al.* 2003) suggested a deficit in deformation in Central Taiwan, prior to the Chi-Chi earthquake (e.g. the map of differential strain shown as figure 7 in Chang *et al.* 2003). Recent insights were obtained from a systematic comparison between the GPS results obtained throughout Taiwan during the 1990–1995 and 2000–2004 periods, in terms of general velocity and deformation patterns relative to the Chinese foreland of Taiwan (Lin *et al.* 2009). This comparison shows that changes are relatively minor near the tips of the Taiwan Island (zones I and V) but large in Central Taiwan (approximately zone III) where velocities have significantly increased in the Chi-Chi earthquake area. This distribution supports the inference presented above, with certainly higher shear strain (mainly right-lateral in zone II and left-lateral in zone IV) and probably accumulating stress in the two intermediate zones between these major domains with contrasting deformation changes.

Although many uncertainties remain, with a dire lack of accurate information about the oldest known earthquakes, a full account and consideration of the earthquake history supported by comparisons with the recent, information-rich instrumental data certainly helps filling the gap between geological information about Pleistocene-Holocene active faults (Ota *et al.* 2005; Chang *et al.* 2000) and the present-day knowledge issued from instrumental seismology.

ACKNOWLEDGMENTS

This study is part of the scientific cooperation between France and Taiwan within the framework of agreements between NSC-IFT-CNRS-Universities (especially National Central University and University of Nice-Sophia Antipolis), including the France–Taiwan Associated International Laboratory 'ADEPT'. The research was supported by the French ANR 'Catell'. It was also supported by the National Sciences Council, under the grant number 96-2119-M-008-013. The senior author benefited from a PhD grant given by the IFT. The authors are deeply indebted to two anonymous reviewers for helpful comments. The authors also thank Dr Chyi-Tyi Lee and Dr Hao Tsu Chu for providing active fault data, as well as Dr N.-G. Hsiao and Dr G.-S. Chang in CWB for valuable information.

REFERENCES

Academia Sinica, Institute of Geophysics, 1970a. *Catalog of Chinese Earthquakes* (in Chinese), p. 361, Academia Sinica, Peking.

Academia Sinica, Institute of Geophysics, 1970b. *Summary of Large Earthquakes in China (from 780 B.C. to February 1970, with magnitude ≥6)* (in Chinese), p. 29, Academia Sinica, Peking.

Academia Sinica, Institute of Geophysics, 1974. *Summary of Large Earthquakes in China (from 780 B.C. to February 1973, with magnitude ≥6)* (in Chinese), p. 31, Academia Sinica, Peking.

Bakun, W.H. & Wentworth, C.M., 1997. Estimating earthquake location and magnitude from seismic intensity data, *Bull. Seism. Soc. Am.*, **87**(6), 1502–1521.

Bakun, W.H., 2005. Magnitude and location of historical earthquakes in Japan and implications for the 1855 Ansei Edo earthquake, *J. Geophys. Res.,* **110,** B02304, doi:10.1029/2004JB003329.

Båth, M., 1981. Earthquake Magnitude—Recent Research and Current Trends, *Earth-Sci. Rev.,* **17,** 315–398.

Benioff, H., 1951. Earthquakes and rock creep, part 1, *Bull. Seism. Soc. Am.,* **44,** 31–62.

Bonilla, M.G., 1975. A Review of Recently Active Faults in Taiwan, U.S. Geol. Survey Open-File Report 75–41.

Central Geological Survey, MOEA, 2005. Active Fault Map of Taiwan, *1 sheet*.

Chang, C.P., Chang, T.Y., Angelier, J., Kao, H., Lee, J.C. & Yu, S.B., 2003. Strain and stress field in Taiwan oblique convergent system: constraints from GPS observation and tectonic data, *Earth Planet. Sci. Lett.,* **214,** 115–127.

Chang, H.C., Lin, C.W., Chan, M.M. & Lu, S.T., 2000. An introduction to the active faults of taiwan: explanatory text of the active fault (in Chinese with English abstract), *Central Geological Survey,*vol. 10, p. 103.

Chang, T.Y., 2002. Seismotectonique de Taiwan (in French), *Ph.D. dissertation*. l'Université P. & M. Curie, Paris, France, 305 pp.

Cheng, S.N. & Yeh, Y.T., 1989. Catalog of the earthquakes in Taiwan from 1604 to 1988 (in Chinese), *Inst. Earth Sci., Acad. Sinica,* IES-R-**661,** 8–10.

Deffontaines, B. et al., 1997. Quaternary transfer faulting in the Taiwan Foothills: evidence from a multisource approach, *Tectonophysics,* **274,** 61–82.

Fang, H., 1969. A compilation of historical records of Taiwan earthquakes before the twentieth century (in Chinese), *Selection of Own Writings on Sixtieth Birthday,* pp. 693–737.

Gutenberg, B. & Richter, C.F., 1942. Earthquake magnitude, *intensity, energy and acceleration, Bull. Seism. Soc. Am.,* **32**(3), 163–191.

Gutenberg, B., 1945. Amplitudes of P, PP and S and magnitude of shallow earthquakes, *Bull. Seism. Soc. Am.,* **35,** 57–69.

Gutenberg, B. & Richter, C.F., 1956a. Magnitude and energy of earthquakes, *Ann. Geofis.,* **9,** 1–15.

Gutenberg, B. & Richter, C.F., 1956b. Earthquake magnitude, intensity, energy and acceleration (second paper), *Bull. Seism. Soc. Am.,* **46,** 105–145.

Hsiao, N.G., 2007. The application of real-time strong-motion observations on the earthquake early warning in Taiwan (in Chinese), *Ph.D. thesis*. National Central University.

Hsieh, Y.S., 1957. A new scale of seismic intensity adapted to the conditions in Chinese territory (in Chinese with English abstract), *Acta Geophys. Sinica,* **6,** 35–47.

Hsu, H., 1983a. Source materials on the history of natural disasters in Ching Taiwan, Disaster Prevention Research Report 72–01, National Science Council, pp. 3–22 (in Chinese).

Hsu, M.T., 1983b. Estimation of earthquake magnitudes and seismic intensities of destructive earthquakes in the Ming and Ching Eras (in Chinese), *Meteorological Report, Taiwan,* **29**(4), 1–18.

Hu, J.C., Yu, S.B., Angelier, J. & Chu, H.T., 2001. Active deformation of Taiwan from GPS measurements and numerical simulations, *J. geophys. Res.,* **106,** 2265–2280.

Hu, J.C. *et al*., 2007. Fault activity and lateral extrusion inferred from velocity field revealed by GPS measurements in the Pingtung area of southwestern Taiwan, *J. Asian Earth Sci.,* **31,** 287–302.

Kanamori, H., 1977. The energy release in great earthquakes, *J. geophys. Res*., **82**(20), 2981–2987.

Kanamori, H., 1978. Quantification of earthquakes, *Nature,* **271,** 411–414.

Kao, H. & Jian, P.R., 2001. Seismogenic patterns in the Taiwan region: Insights from source parameter inversion of BATS data, *Tectonophysics,* **333,** 179–198.

Kao, H., Liu, Y.-H. & Jian, P.-R., 2001. Source parameters of regional earthquakes in Taiwan: January-December 1997, *Terr. Atmos. Oceanic Sci.,* **12,** 431–439.

Kawasumi, H., 1943. Intensity and magnitude (in Japanese), *Zisin,* **15,** 6–12.

Lee, W.H.K., Wu, F.T. & Jacobsen, C., 1976. A catalog of historical earthquakes in China complied from recent Chinese publications, *Bull. Seism. Soc. Am.,* **66**(6), 2003–2016.

Lin, K.C., Hu, J.C., Ching, K.E., Angelier, J., Rau, R.J., Tsai, C.H., Shin, T.C. & Huang, M.H., 2009. Current crustal deformation and strain rate as deduced from continuous GPS measurements in Taiwan, submitted.

Omori, F., 1907a. Earthquake of the Chiayi area, *Taiwan, 1906: Introduction of Earthquake,* pp. 103–147 (in Japanese).

Omori, F., 1907b. Preliminary note on the Formosa earthquake of March 17, *1906: Bull. Imp. Earthquake Investigation Committee,* **1**(2), 53–69.

Ota, Y., Chen, Y.G. & Chen, W.S., 2005. Review of paleoseismological and active faults studies in Taiwan in the light of the Chichi earthquake of September 21, 1999, *Tectonophysics,* **408,** 63–77.

Richter, C.F., 1935. An instrumental earthquake magnitude scale, *Bull. Seism. Soc. Am,* **25,** 1–32.

Richter, C.F., 1958. *Elementary Seismology,* 768 pp., W.H. Freeman, San Francisco.

Shin, T.C., Tsai, Y.B. & Wu, Y.M., 1996. Rapid response of large earthquakes in Taiwan using a realtime telemetered network of digital accelerographs, in *Proceedings of the 11th World Conference on Earthquake Engineering*, Acapulco, Mexico, Paper no. 2137.

Shin, T.C. & Chang, G.S., 2005. *Taiwan Earthquake Observation System, 921 Chi-Chi Earthquake,* National Science Council, pp. 43–59 (in Chinese).

Stefánsson, R. & Halldórsson, P., 1988. Strain release and strain build-up in the south Iceland seismic zone, *Tectonophysics,* **152,** 267–276.

Suppe, J., 1981. Mechanics of mountain building and metamorphism in Taiwan, *Geol. Soc. China Memoir,* **4,** 67–89.

Suppe, J., 1984. Kinematics of arc-continent collision, flipping of subduction and back-arc spreading near Taiwan, *Geol. Soc. China Memoir,* **6,** 21–33.

Tsai, Y.B., 1985. A study of disastrous earthquakes in Taiwan, 1683–1895, *Bull. Inst. Earth Sc., Acad. Sin.,* **5,** 1–44.

Wang, J.H., 1992. Magnitude scales and their relations for Taiwan earthquakes: a review, *Terr. Atmos. Oceanic Sci.,* **3,** 449–468.

Wessel, P. & Smith, W.H.F., 1995. New version of the generic mapping tools released: EOS trans., *AGU,* **76,** 329.

Wu, Y.M., Chen, C.C., Shin, T.C., Tsai, Y.B., Lee, W.H.K. & Teng, T.L., 1997. Taiwan Rapid Earthquake Information Release System, *Seism. Res. Lett.,* **68,** 931–943.

Yeh, Y.T., Cheng, S.N., Hu, Y.K., Shin, T.C. & Chen, T.G., 1994. Estimation of the location and the magnitude of several earthquakes catalogue in the region of Taiwan (II), Bull. Technique Report on Seism. Central Weather Bureau 8–2, 219–238 (in Chinese).

Yu, S.B. & Chen, H.Y., 1994. Global positioning system measurements of crustal deformation in the Taiwan arc-continent collision zone, *Terr. Atmos. Oceanic Sci.,* **5,** 477–498.

Yu, S.B., Chen, H.Y. & Kuo, L.C., 1997. Velocity field of GPS stations in the Taiwan area, *Tectonophysics,* **274,** 41–59.

Yu, S.B., Kuo, L.C., Punongbayan, R.S. & Ramos, E.G., 1999. GPS observation of crustal motion in the Taiwan-Luzon region, *Geophys. Res. Lett.,* **26**(7), 923–926.